applied sciences

MDPI

Article

Investigating the Ability of the Tooth and Surrounding Support Tissues to Absorb and Dissipate Orthodontic Loads during Periodontal Breakdown—Finite Elements Analysis

Radu-Andrei Moga [1,*], Cristian Doru Olteanu [2,*] and Ada Gabriela Delean [1]

[1] Department of Cariology, Endodontics and Oral Pathology, School of Dental Medicine, University of Medicine and Pharmacy Iuliu Hatieganu, Str. Motilor 33, 400001 Cluj-Napoca, Romania; ada.delean@umfcluj.ro
[2] Department of Orthodontics, School of Dental Medicine, University of Medicine and Pharmacy Iuliu Hatieganu, Str. Avram Iancu 31, 400083 Cluj-Napoca, Romania
* Correspondence: andrei.moga@umfcluj.ro (R.-A.M.); olteanu.cristian@umfcluj.ro (C.D.O.)

Featured Application: For an orthodontist practitioner, quantification of the absorption–dissipation ability of dental tissues is of extreme importance since there is a constant danger when applying loads to produce ischemia and further resorptive processes (e.g., 0.6–1.2 N vs. 2.4 N). Orthodontic treatment is not always performed in intact periodontium; thus, it must be emphasized that in reduced periodontium, there are biomechanical changes that if not acknowledged could compromise treatment prognosis. The study is the first to analyze not only the absorption–dissipation issues, but also to investigate how the biomechanical behavior is affected by bone loss. For researchers, this study not only approaches the technical issues related to the numerical studies methodology, but also clears some aspects that could significantly influence the results accuracy. Herein, the analysis proves that the tooth absorbs and dissipates most of the stress due to applied forces (high percentage variability), in both intact and reduced periodontium, acting as a single-stand continuum structure, with enamel having a similar absorption–dissipation ability as dentine (both behaving in a similar way to ductile materials). All other tissular components have a constant absorption–dissipation ability, that changes very little during periodontal breakdown. It has also been proven that some of the movements are more stressful (i.e., rotation and translation) than the others (tipping, intrusion, and extrusion). The analysis herein showed that the assumed boundary conditions (linear elasticity, isotropy, and homogeneity) widely used in dental studies, are correct up to 2.4 N of loads when Tresca failure criterion is employed.

Abstract: Herein, the finite elements analysis (FEA) numerical study investigated the absorption–dissipation ability of dental tissues under orthodontic forces, during orthodontic movements and the periodontal breakdown process. Additionally, we investigated the correctness of FEA boundary assumptions up to 2.4 N of loads. Eighty-one models of the second lower premolar were subjected to 810 FEA numerical simulations using Tresca failure criterion under 0.6 N, 1.2 N, and 2.4 N and five movements: intrusion, extrusion, rotation, tipping, and translation. The results showed that both coronal dentine and enamel components had comparable high absorption–dissipation abilities, allowing for only a limited fraction of stresses to reach the circulatory sensitive tissues. Isotropy, linear elasticity, and homogeneity are correct when Tresca is employed up to 2.4 N. Forces of 0.6 N, 1.2 N, and 2.4 N displayed similar qualitative results for all movements and bone levels, while quantitative results doubled for 1.2 N and quadrupled for 2.4 N when compared with 0.6 N. FEA simulations showed 0.6–1.2 N to be safe for application in intact periodontium, while for reduced periodontium more than 0.6 N are prone to resorptive and ischemic risks. For reducing these risks, after 4 mm of bone loss, 0.2–0.6 N are recommended. Rotation and translation were the most stressful followed by tipping.

Keywords: tooth; enamel; dentin; periodontal breakdown; finite elements analysis; failure criteria selection; orthodontic movements

Citation: Moga, R.-A.; Olteanu, C.D.; Delean, A.G. Investigating the Ability of the Tooth and Surrounding Support Tissues to Absorb and Dissipate Orthodontic Loads during Periodontal Breakdown—Finite Elements Analysis. *Appl. Sci.* **2024**, *14*, 1041. https://doi.org/10.3390/app14031041

Academic Editor: Irene Pina-Vaz

Received: 3 January 2024
Revised: 22 January 2024
Accepted: 24 January 2024
Published: 25 January 2024

1. Introduction

Dental tissues are subjected to various levels of stress during the application of orthodontic loads. The first tissues that are subjected to orthodontic stresses are bracket, enamel, and dentine. Some of the stresses are absorbed and dissipated through these components, and only a part reaches other tissular components (i.e., periodontal ligament, PDL; neuro-vascular bundle, NVB; dental pulp; cortical and trabecular bone). This absorption–dissipation ability is theoretically and clinically recognized, but not yet quantified or sufficiently studied [1–4].

Some of the dental tissular components are more sensitive to the orthodontic pressures due to a better circulatory vessel system (i.e., PDL, NVB, and dental pulp); thus, the physiological maximum hydrostatic pressure MHP of 16 KPa (approx. 80% of systolic pressure) is exceeded and both ischemic and resorptive risks are inevitable [5,6].

Tissular absorption–dissipation ability is based on the internal micro-architecture of the tooth and supporting tissues, individual components, and the way they biomechanically behave under stresses.

The material of bracket (i.e., stainless steel) is a ductile material that can deform under loads and recover its initial shape when the loads ceased [7–9].

From a mechanical point-of-view (according to the material failure theory), a ductile material (e.g., steel and rubber) can suffer from various elastic deformations (higher tensile resistance) before its failure and could return to its original form when the force ceased. On the other hand, a classical brittle material (e.g., concrete and glass), when subjected to loads, suffers from limited deformations, closely followed by cracking and fracture, but with a higher compression resistance [9,10].

Enamel, considered as the hardest tissue, has an internal micro-architecture that is made of hexagonal-prism-shaped rods [1,11,12]. As a brittle material, when subjected to loads, the enamel should not deform, but rather should crack/fissure. However, clinically, this type of behavior is neither confirmed nor studied. Therefore, based on only clinical acknowledged behavior, the internal micro-architecture seems to suffer from some recoverable deformations, making it a ductile-like material with a certain brittle flow mode [10].

The dentine component (which resembles a ductile material) is the largest component in the tooth structure, with an internal micro-architecture made of oriented tubules surrounded by a highly mineralized cuff of peritubular dentin and inter-tubular matrix of type I collagen fibrils reinforced with hydroxyapatite [11,13]. Dentine is recognized for having the ability to absorb–dissipate both orthodontic and bite loads, while its physical properties vary depending on topography (i.e., anisotropy) [1,11,13].

Dental pulp and neuro-vascular bundle (NVB) are ductile-like materials [2], being highly vascularized tissues, with NVB being more sensitive to circulatory disturbances due to its topographical position in the apical third PDL [2,5].

Cementum (which resembles a ductile material) has similar physical properties to dentine and ensures the support and absorption–dissipation of both tissues [1,2,10,11,14].

The internal micro-architecture of PDL (which resembles a ductile material) comprises collagen fibers displayed as variously orientated dense fiber bundles that fill the spaces between the bone and cementum by 0.4–1.5 mm [3]. PDL along with NVB are the most sensitive to circulatory disturbance tissues due to a well-represented vascular support including apical vessels, perforating vessels, and gingival vessels. The outward-facing blood vessels are involved in biomechanical suspension and absorption–dissipation ability, while those facing inwards are involved in nutritional metabolism [3].

Bone (cortical and trabecular/cancellous components) behave as a continuum and single-stand structure with high adaptation ability of changing the shape to provide the strongest structure with a minimum of volume and resemblance to ductile materials [15–20].

All dental tissular components are anisotropic and non-homogenous materials (i.e., variable physical properties on different directions depending on circumstances) [16,19], do not obey Hooke's law [1], and with non-linear elastic behavior. These issues must be

clearly addressed in every numerical study due to their significant influence over the results accuracy.

The acknowledged dental components' physical properties are: cortical bone—16.7 GPa of compressive modulus and 157 MPa of compressive strength; trabecular/cancellous bone—0.155 GPa of compressive modulus and 6 MPa of compressive strength [19–27]; enamel—62.2 MPa of compressive stress [1], 11.5–42.1 MPa of maximum tensile strength [11], and 53.9–104 MPa of maximum shear stress [13]; dentine—29–73.1 MPa of maximum shear stress; enamel–dentine—53.9–104 MPa of maximum shear stress [13].

If the tooth's surrounding support system is intact, common orthodontic forces up to 1.2 N [4] are safely applied. However, when there are various levels of bone loss, due to mechanical changes, the stress absorption–dissipation ability changes, with higher ischemic and resorptive risks and altered treatment prognosis [5,6,10]. When analyzing small movements under light forces, the issue related to the loading conditions must be carefully addressed. For predictable results, both intensity of the force and orthodontic strength must be addressed, as well as time and amplitude. The intensity is the power transferred per unit area (extremely important for small loads applied on small surface areas), while the strength is the capacity of an object—to withstand force/pressure, particularly the maximum load a material can sustain before yielding. To keep the intensity of the force constant for each orthodontic movement, the surface of the applied loads must be carefully measured, as well as the direction of the force (i.e., X-Y-Z spatial directions) since it directly influences the discharged area. The orthodontic strength of the materials and dental tissues must be higher than the stress manifested during the orthodontic movement. The time of the applied load is also important to simulate, as closely as possible, the biomechanical behavioral response of human dental tissues.

There is only one single available method for the study of stress distribution in dental tissues, the finite elements analysis (FEA), which individually investigates the stress distribution and biomechanical behavior of each dental component [5,6,10]. In dental field, the numerical studies' results are regarded with care since they often contradicted clinical knowledge and displayed various results from one report to another [19–47]. This issue was not addressed, except for our previous research [5,6,9,10,16,48].

FEA accuracy depends on the selection of proper failure criteria which are suitable for the analyzed material, anatomically correct models, and proper boundary conditions. Our previous studies [5,6,9,10,16,48] reported that since dental tissues are ductile-like materials (with a certain brittle flow mode) only a failure criterion specially designed for ductile materials is suitable (i.e., Von Mises overall stress and Tresca shear stress). Moreover, for validation, the quantitative results must be correlated with MHP, while qualitative results with acknowledged clinical data. Despite many FEA studies [19–47,49,50] investigating PDL and bone–implant interface, none approached these vital issues, thereby supplying questionable and contradictory results [5,6,9,10,16,48]. Only one older numerical FEA study [30] was found to make a limited distinction between brittleness and ductileness for the root canal filling, but without further development.

Most of the recent FEA studies [28–41,43,44,49–51] employed the hydrostatic pressure criterion (specially designed for liquids, with no shear stress), maximum principal S1 tensile stress, and minimum principal S3 compressive stress (for brittle-like materials) for the study of PDL (a ductile-like material), while the reported results invariably exceeded MHP even for light orthodontic forces (suggesting ischemic and resorptive risks that contradict clinical data).

The bone–implant [19–26,44] and bone–tooth [29,43,44] FEA studies employed S1–S3 (brittle-like) and Von Mises (ductile-like) failure criterion but without any discussion about the above-mentioned issues.

Most of the above FEA studies employed included boundary conditions isotropy, linear elasticity, and homogeneity, despite the anatomical tissues being none of these, without addressing their suitability, adequacy, and influence over the results accuracy issues. Moreover, the applied forces were higher than 1.2 N (despite the above boundary conditions

being correct only for small displacements and applied forces), while the investigated models were artificially created and anatomically simplified (i.e., lower number of nodes and elements with a higher global element size) [19–47,49,50]. It must be emphasized that, from a biomechanical point-of-view, linear elasticity and isotropy assumptions are correctly employed only if the applied forces are up to 1 N, and the non-homogeneity of materials is considered and addressed using the Tresca criterion. There is no available data on the above issues for higher applied forces in dental tissues and no studies, except for our previous studies [2,3,5,6,9,10,16,48], acknowledged and addressed these issues.

Herein, the study aimed to individually assess the biomechanical absorption–dissipation ability of dental tissues in intact periodontium under 0.6 N, 1.2 N, and 2.4 N during the five most used orthodontic movements, as well as the changes produced by the reduction in supporting tissues during a gradual horizontal periodontal breakdown of 1–8 mm. Additionally, we investigated the suitability and biomechanical behavioral correctness of the frequently employed boundary conditions (isotropy, linear elasticity, and homogeneity) under increasing loads.

2. Materials and Methods

This numerical FEA analysis is part of a larger step-by-step research project [2,3,5,6,9,10,16,48] (with clinical protocol no. 158/02.04.2018) investigating the FEA methodology to improve the accuracy of numerical study results and to assess the biomechanical behavioral changes in dental tissues produced by the periodontal breakdown.

Herein, the study performed 810 numerical simulations on 81 models of the lower premolar from nine patients (with mean age 29.81 $\pm$ 1.45 years, four males, five females, oral informed consent); thus, a sample size of nine. Nevertheless, it must be emphasized that all FEA numerical studies mentioned above used a sample size of one (one patient, one model, and a few numerical simulations). Thus, the sample size used here was found to be acceptable.

Initially, more patients were examined, but only nine met the inclusion criteria (intact mandibular arch, intact teeth, no malposition, non-inflamed periodontium, no advanced bone loss, orthodontic treatment indication, regular follow-up availability, good oral hygiene). The exclusion criteria were in opposition to the above.

The mandibular region with two molars and premolars received a CBCT examination (cone beam computed tomography, ProMax 3DS, Planmeca, FI-00880 Helsinki, Finland, 0.075 mm voxel size). The DICOM slices containing various shades of gray were loaded in Amira 5.4.0 (Visage Imaging Inc., 300 Brickstone Square, Suite 201, Andover, MA 01810, USA) reconstruction software. The reconstruction process was manual since the automated software function did not correctly identify all tissular components, thereby enhancing the anatomical accuracy of the models.

Only the second lower premolar was reconstructed, while the alveolar bone socket of the other three teeth was filled with bone (cortical and trabecular). All dental tissue components were identified and reconstructed: enamel, dentine, dental pulp, neuro-vascular bundle (NVB), periodontal ligament (PDL), cortical and trabecular bone (Figure 1).

Cementum could not be separated from dentine; thus, due to the similar physical properties, it was reconstructed as dentine. PDL had a variable thickness of 0.15–0.225 mm and included NVB in its apical third. The base of a stainless-steel bracket was reconstructed on the enamel component. Since the models had various but small levels of bone loss, limited to cervical third, the missing bone and PDL were reconstructed, thus obtaining nine models with intact periodontium of 5.06–6.05 million C3D4 tetrahedral elements, 0.97–1.07 million nodes, and a global element size of 0.08–0.116 mm (high anatomical accuracy, when compared with the above-mentioned numerical studies). Due to the manual reconstruction process, all models displayed a small number of surface irregularities in non-essential areas (the stressed areas were quasi-continuous). All internal mesh testing for verifying the algorithm base processes in both software resulted in no mesh/element errors, with only a limited number of element warnings (Figure 2, yellow dots). Thus, for one of

the intact periodontium nine models from a total number of 5.06–6.05 million elements, there were only 264 element warnings (representing 0.0043%): 201 (0.0039%) of 5,117,355 bone structure elements, 63 (0.00677%) of 930,023 of tooth, bracket, and PDL elements, 39 (0.00586%) of 665,501 tooth and bracket elements, 26 (0.00459185%) of 566,221 radicular dentine–cementum and coronal dentine elements, and 17 (0.0141469%) of 120,168 enamel and bracket elements (Figure 2).

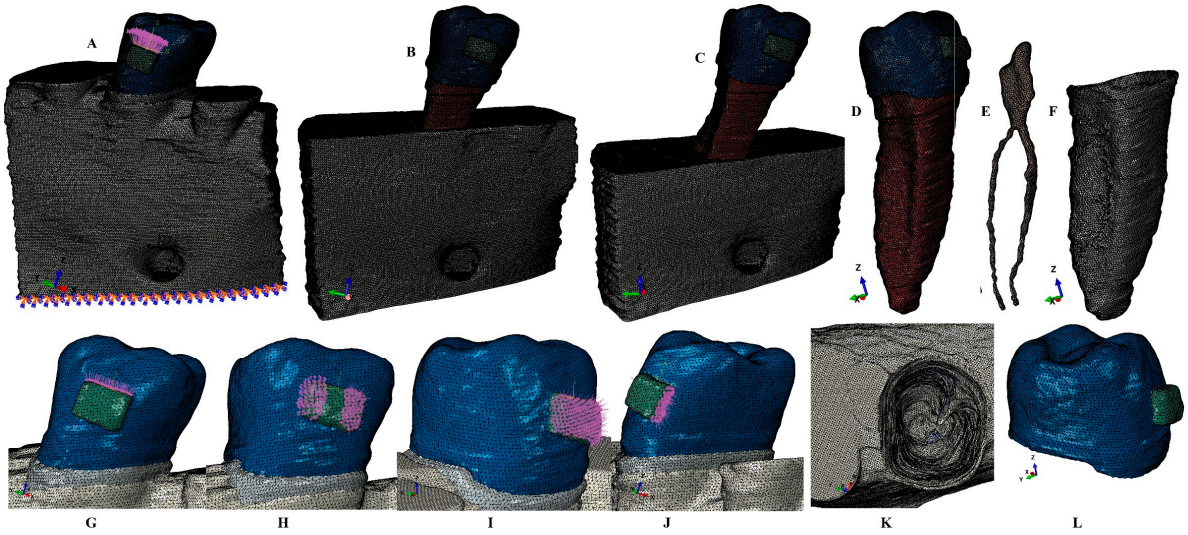

Figure 1. Mesh model: (**A**)—second lower right premolar model with 0 mm bone loss and applied vector for extrusion, (**B**)—second lower right premolar model with 4 mm bone loss, (**C**)—second lower right premolar model with 8 mm bone loss, (**D**)—second lower right premolar model, (**E**)—dental pulp and NVB, (**F**)—PDL, applied vectors: (**G**)—intrusion, (**H**)—rotation, (**I**)—tipping, (**J**)—translation, (**K**)—alveolar bone socket, (**L**)—enamel with stainless-steel bracket base.

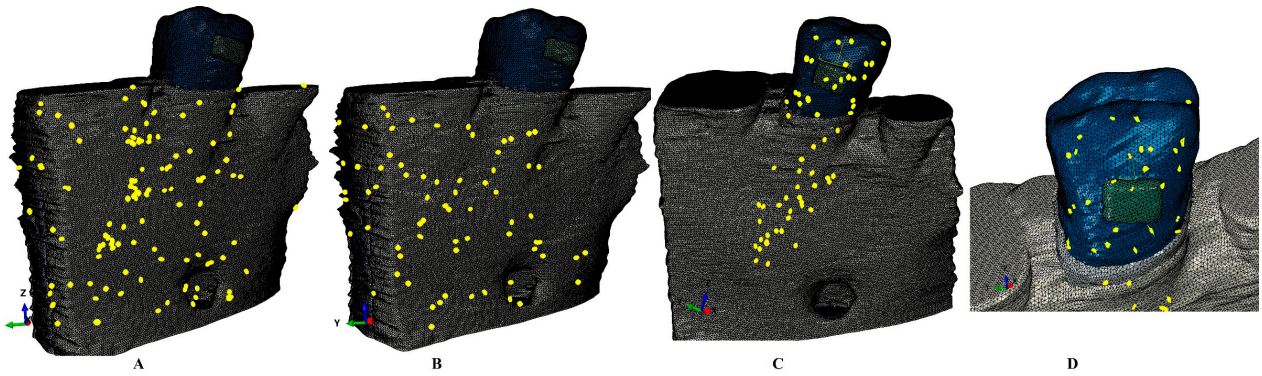

Figure 2. Element warnings in one of nine intact periodontium models: (**A**)—cortical component, (**B**)—trabecular component, (**C**)—tooth structure, (**D**)—tooth structure (details).

A gradual horizontal periodontal breakdown process (0–8 mm) was simulated by reducing the bone and PDL by 1 mm, thus obtaining eighty-one models.

All numerical simulations were performed using Abaqus 6.13-1 software (Dassault Systèmes Simulia Corp., Stationsplein 8-K, 6221 BT Maastricht, The Netherlands). The boundary conditions were isotropy, linear elasticity, and homogeneity (similar to the above-mentioned numerical studies, Table 1). Tresca failure criterion (maximum shear stress, specially designed for non-homogenous ductile materials with a certain brittle flow mode) was employed.

Table 1. Elastic properties of materials.

Material	Young's Modulus, E (GPa)	Poisson Ratio, υ	Refs.
Enamel	80	0.33	[2,3,5,6,9,10,16,48]
Dentin/Cementum	18.6	0.31	[2,3,5,6,9,10,16,48]
Pulp	0.0021	0.45	[2,3,5,6,9,10,16,48]
PDL	0.0667	0.49	[2,3,5,6,9,10,16,48]
Cortical bone	14.5	0.323	[2,3,5,6,9,10,16,48]
Trabecular bone	1.37	0.3	[2,3,5,6,9,10,16,48]
Bracket (Stainless Steel)	190	0.265	[2,3,5,6,9,10,16,48]

Three orthodontic forces, 0.6 N (approx. 60 gf), 1.2 N (approx. 120 gf), and 2.4 N (approx. 240 gf), were applied at the stainless-steel bracket base (on various surfaces) for simulating the five most used orthodontic movements: extrusion, intrusion, rotation, tipping, and translation. To keep the intensity of the force constant, the surface of the applied area was carefully considered for each movement (i.e., magnitude). In particular, the loads were adapted depending on each surface-measured area to keep the load constant and uniform. Abaqus load manager conditions include step procedure: static, general; load type: pressure; load status: created in step; distribution: uniform; magnitude: depending on the surface area; amplitude: ramp. Abaqus boundary manager conditions include step procedure: static, general; boundary condition type: symmetry/antisymmetry/encastre; boundary condition status: created in step. When editing the load appliance, the chosen distribution was uniform and the amplitude was "Ramp" (i.e., default)—the load was applied with increasing small increments up to the total amount of force. The load appliance was continuous with a small incremental progressive increase. Since deformations were extremely small as well as the amount of loads, with or without activating "follow the nodal rotation function", the results will be similar.

The first two loads were selected since they are considered safe for use in intact periodontium and for being able to correlate them with our previous research and the above-mentioned numerical studies. The third load (2.4 N) was chosen since it is higher than the mechanical limit of 1 N, to investigate the differences between the results (to assess the assumed boundary conditions), and to be able to correlate them with the above-mentioned numerical results.

The numerical simulation results were both qualitative (color-coded projections of various colors of the maximum shear stress with high stress—red-orange, moderate stress: yellow-green, and low stress: blue) and quantitative (average numerical values in KPa). These results were then correlated with the 16 KPa of physiological MHP, mechanical knowledge, acknowledged clinical data, and other similar numerical analyses.

3. Results

Herein, the numerical simulation analyzed 81 3D models in 810 simulations. No visible influence of age, periodontal status, or gender was seen. The results were both qualitative (color-coded projections of the maximum shear stress distribution in all models' components, Figures 3–8) and quantitative (Tables 2–7, in KPa).

All three forces (0.6 N, 1.2 N, and 2.4 N) displayed similar qualitative results (independently of bone loss level), while the quantitative results doubled for 1.2 N and quadrupled for 2.4 N when compared with 0.6 N.

Quantitatively, the highest amount of stress was displayed by rotation and translation, followed by tipping, while intrusion and extrusion were the least stressful.

3.1. Extrusion (Figure 3, Table 2)

Quantitatively, in intact periodontium, 0.6 N produced the highest amount of stress (i.e., 299.4 KPa, Figure 3A and Table 2) at bracket level, with a visible decreasing pattern in the other components. Qualitatively, the highest stress concentrated on and around the bracket (Figure 3B,C). However, when individually assessing each component, the most heavily stressed were dentin (Figure 3D), NVB (Figure 3E), and PDL (Figure 3F). In the

dentine–cementum component, the vestibular cervical third displayed orange-yellow high stress areas, which are prone to external root resorption risks (i.e., 107.5 KPa, 6.7 times higher than the physiological MHP of 16 KPa). Qualitatively, despite the fact that PDL, pulp, and NVB displayed red-orange high stress areas, they did not quantitatively exceed MHP; thus, they can be safely applied in intact periodontium (Table 2). Moreover, despite the fact that bone and dentine–cementum (due to lesser vascularization) components exceeded MHP, they are not as sensitive to high pressures; thus, the resorptive and ischemic risks are smaller. The absorption–dissipation ability pattern of the above structures was clearly visible (Table 2): a progressive decrease in stress in radicular dentine (14.76–35.9%), alveolar bone socket (12.51–50.04%), PDL (1–2.24%), pulp (0.05%), and NVB (0.57%) when compared with the initial stress applied on the bracket (299.4 KPa).

In reduced periodontium (1–8 mm), the quantitative amount increases in correlation with bone loss. Nevertheless, the decreasing stress pattern (i.e., absorption–dissipation ability) in the model's components, which is visible in intact periodontium, was maintained. Qualitatively and quantitatively, coronal stress around and on the bracket increases (red-orange visible in Figure 3B,C), while radicular stress (Figure 3D) extends in the entire root (i.e., visible external resorptive risk areas are in the middle third). The progression of bone loss increases stresses in the entire alveolar socket (Figure 3G) and PDL (Figure 3F). Quantitatively, 0.6 N induces stresses in PDL cervical third exceeding MHP after 6 mm of loss, with higher ischemic and resorptive risks. From stresses manifested on the bracket level (305.5–392.5 KPa), only 1.24–5.75% was displayed in PDL, 0.05–0.09% in dental pulp, 0.63–1.11% in NVB, 14–50% in alveolar socket bone, and 24.51–63.47% in radicular dentine (Table 2). There was a visible increasing stress pattern in radicular dentine component from 24.51–42.77% in 1 mm loss to 63.47% in 8 mm loss, which is strictly correlated with periodontal breakdown.

The bracket absorption–dissipation ability (difference between tooth with bracket and without bracket coronal stress) was 15.48% in 0 mm, 16.43% in 1 mm, and 4.02% in 8 mm loss.

The enamel absorption–dissipation ability (difference between coronal tooth without bracket and coronal dentine stress) was 62.26% in 0 mm, 62.26% in 1 mm, and 65.44% in 8 mm loss.

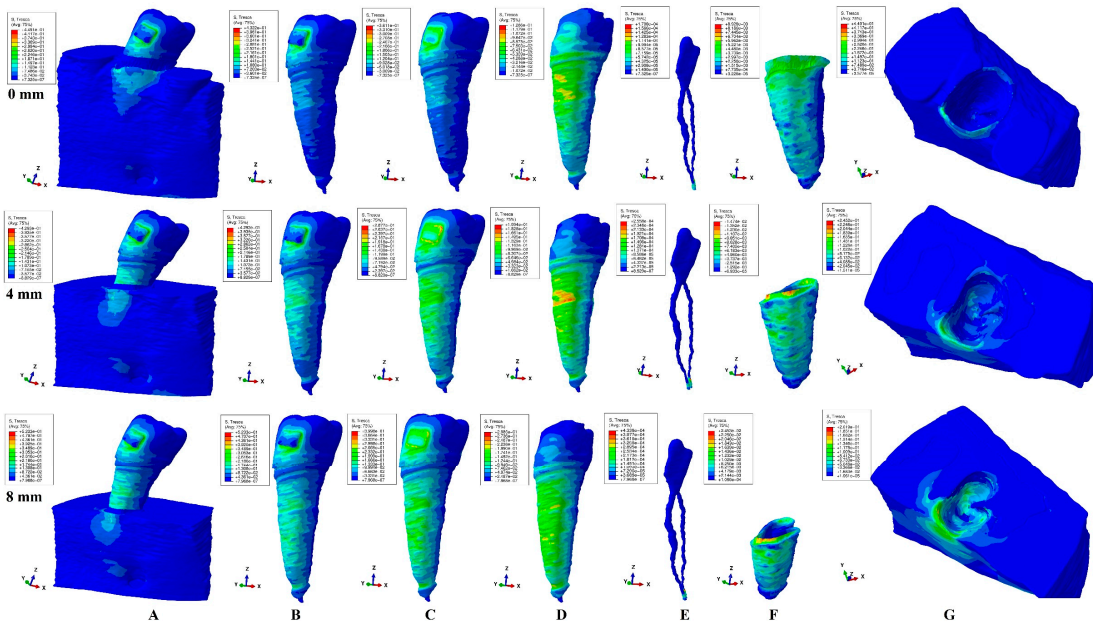

Figure 3. Extrusion—Tresca stress display in dental tissues subjected to 0.6 N for 0, 4, and 8 mm bone loss: (**A**)—dental tissues' structure, (**B**)—tooth with bracket, (**C**)—tooth without bracket, (**D**)—dentine component, (**E**)—dental pulp and NVB, (**F**)—PDL, (**G**)—bone with alveolar socket.

Table 2. Maximum stress average values (KPa) produced by orthodontic forces in tooth structure and dentine–cementum.

Resorption (mm)			**0**	**1**	**2**	**3**	**4**	**5**	**6**	**7**	**8**
Extrusion	Structure		**299.40**	**305.05**	**310.70**	**316.35**	**322.00**	**339.60**	**357.25**	**374.87**	**392.50**
0.6 N/60 gf	Tooth + bracket	a	72.03	107.67	143.31	178.98	214.60	237.27	259.94	282.61	305.30
Stress		m	108.00	134.65	161.30	187.95	214.60	237.27	259.94	282.61	305.30
Amount		c	216.10	233.63	251.15	268.67	286.20	290.97	295.75	300.52	305.30
In each		C	288.10	296.57	305.00	313.52	322.00	328.72	335.45	342.17	348.90
Component	Tooth	a	60.18	93.08	125.98	158.88	191.80	210.50	229.20	247.90	266.60
		m	90.28	115.66	141.04	166.42	191.80	210.50	229.20	247.90	266.60
		c	120.40	144.20	168.00	191.80	215.63	228.37	241.11	253.85	266.60
		C	240.70	246.45	252.20	257.95	263.70	281.05	298.40	315.75	333.10
	Dentine	a	44.18	74.76	105.34	135.92	166.50	187.15	207.81	228.46	249.11
		m	44.18	74.76	105.34	135.92	166.50	187.15	207.81	228.46	249.11
		c	107.50	130.48	153.45	176.43	199.40	211.83	224.26	236.68	249.11
		C	54.28	57.66	61.04	64.41	67.79	69.88	71.97	74.06	76.15
	Bone	a	37.46	43.43	49.40	55.36	61.33	62.82	64.31	65.80	67.30
		m	37.46	38.32	39.17	40.02	40.89	43.27	45.67	48.00	50.47
		c	149.83	153.25	156.67	160.09	163.51	164.71	165.92	167.12	168.34
	NVB	NVB	1.71	1.92	2.14	2.35	2.56	3.01	3.45	3.90	4.34
	Pulp	a	0.15	0.17	0.19	0.20	0.22	0.26	0.30	0.33	0.37
		c	0.15	0.17	0.19	0.20	0.22	0.26	0.30	0.33	0.37
	PDL	a	3.00	3.80	4.59	5.39	6.18	6.70	7.22	7.73	8.25
		m	3.00	3.80	4.59	5.39	6.18	6.70	7.22	7.73	8.25
		c	6.70	8.41	10.11	11.82	13.52	15.77	18.04	20.29	22.55
Extrusion	Structure %		**100**	**100**	**100**	**100**	**100**	**100**	**100**	**100**	**100**
0.6 N/60 gf	Tooth + bracket %	a	**24.06**	**35.30**	**46.12**	**56.58**	**66.65**	**69.87**	**72.76**	**75.39**	**77.78**
Stress %		m	36.07	44.14	51.92	59.41	66.65	69.87	72.76	75.39	77.78
Reaching		c	72.18	76.59	80.83	84.93	88.88	85.68	82.79	80.17	77.78
Each		C	**96.23**	**97.22**	**98.17**	**99.11**	**100.00**	**96.80**	**93.90**	**91.28**	**88.89**
Component	Tooth %	a	**20.10**	**30.51**	**40.55**	**50.22**	**59.57**	**61.98**	**64.16**	**66.13**	**67.92**
		m	30.15	37.92	45.39	52.61	59.57	61.98	64.16	66.13	67.92
		c	40.21	47.27	54.07	60.63	66.96	67.25	67.49	67.72	67.92
		C	**80.39**	**80.79**	**81.17**	**81.54**	**81.89**	**82.76**	**83.53**	**84.23**	**84.87**
	Dentine %	a	**14.76**	**24.51**	**33.90**	**42.97**	**51.71**	**55.11**	**58.17**	**60.94**	**63.47**
		m	14.76	24.51	33.90	42.97	51.71	55.11	58.17	60.94	63.47
		c	35.91	42.77	49.39	55.77	61.93	62.38	62.77	63.14	63.47
		C	**18.13**	**18.90**	**19.64**	**20.36**	**21.05**	**20.58**	**20.15**	**19.76**	**19.40**
	Bone %	a	**12.51**	**14.24**	**15.90**	**17.50**	**19.05**	**18.50**	**18.00**	**17.55**	**17.15**
		m	12.51	12.56	12.61	12.65	12.70	12.74	12.78	12.80	12.86
		c	**50.04**	**50.24**	**50.43**	**50.61**	**50.78**	**48.50**	**46.44**	**44.58**	**42.89**
	NVB %	NVB	**0.57**	**0.63**	**0.69**	**0.74**	**0.79**	**0.89**	**0.97**	**1.04**	**1.11**
	Pulp %	a	**0.05**	**0.05**	**0.06**	**0.06**	**0.07**	**0.08**	**0.08**	**0.09**	**0.09**
		c	**0.05**	**0.05**	**0.06**	**0.06**	**0.07**	**0.08**	**0.08**	**0.09**	**0.09**
	PDL %	a	**1.00**	**1.24**	**1.48**	**1.70**	**1.92**	**1.97**	**2.02**	**2.06**	**2.10**
		m	1.00	1.24	1.48	1.70	1.92	1.97	2.02	2.06	2.10
		c	**2.24**	**2.76**	**3.25**	**3.73**	**4.20**	**4.64**	**5.05**	**5.41**	**5.75**

structure—stress displayed by the 3D model. Tooth + bracket, Tooth, Dentine, Bone, NVB, Pulp, PDL components—stress displayed by these components. a—apical third, m—middle third, c—cervical third, C—crown. Tooth + bracket %, Tooth %, Dentine %, Bone %, NVB %, Pulp %, PDL % components—% stress displayed by these components.

3.2. Intrusion (Figure 4, Table 3)

In intact and reduced periodontium, both qualitative and quantitative biomechanical behaviors are similar to extrusion. However, there are some visible differences (smaller amount of stress in cervical third) in PDL component, which are specific to the intrusion movement (Figure 4F).

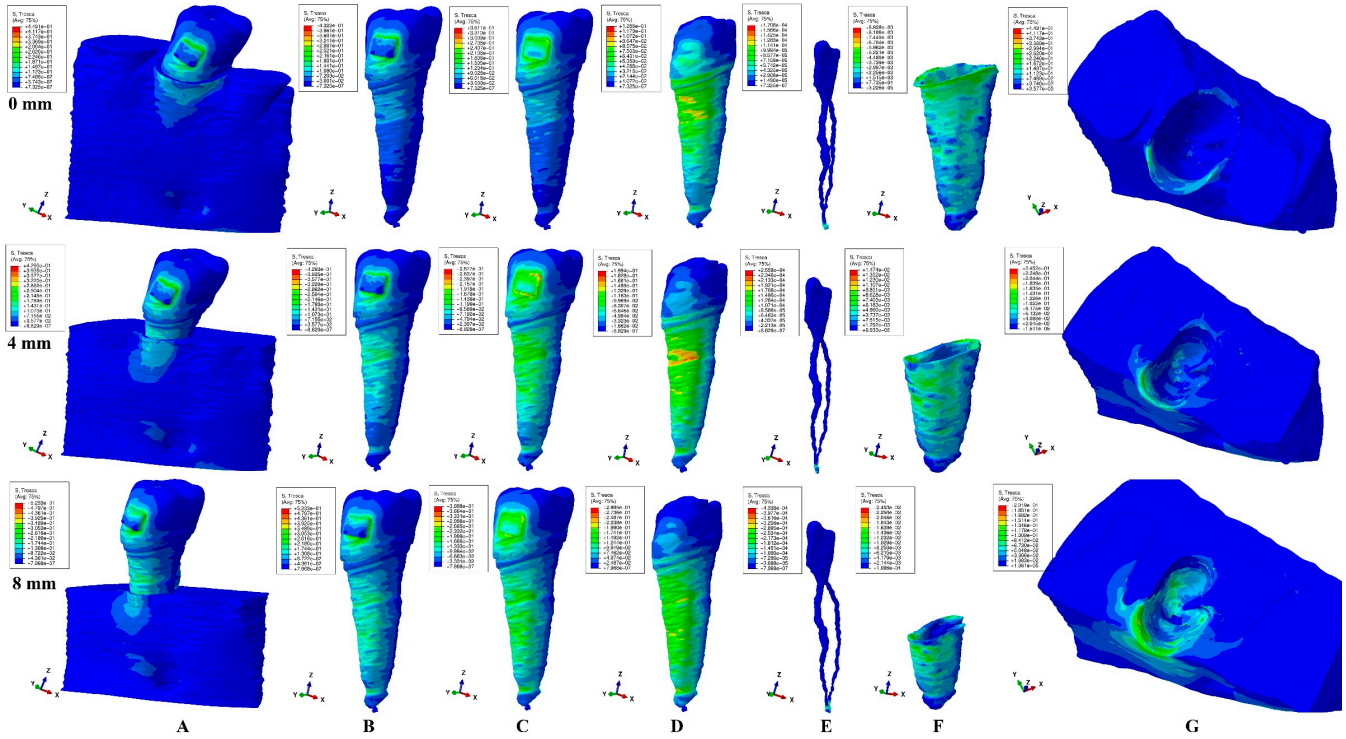

Figure 4. Intrusion—Tresca stress display in dental tissues subjected to 0.6 N for 0, 4, and 8 mm bone loss: (**A**)—dental tissues' structure, (**B**)—tooth with bracket, (**C**)—tooth without bracket, (**D**)—dentine component, (**E**)—dental pulp and NVB, (**F**)—PDL, (**G**)—bone with alveolar socket.

Table 3. Maximum stress average values (KPa) produced by orthodontic forces in tooth structure and dentine–cementum.

Resorption (mm)			**0**	**1**	**2**	**3**	**4**	**5**	**6**	**7**	**8**
Intrusion	Structure		**299.40**	**305.05**	**310.70**	**316.35**	**322.00**	**339.60**	**357.25**	**374.87**	**392.50**
0.6 N/60 gf	Tooth + bracket	a	72.03	107.67	143.31	178.98	214.60	237.27	259.94	282.61	305.30
Stress		m	108.00	134.65	161.30	187.95	214.60	237.27	259.94	282.61	305.30
Amount		c	216.10	233.63	251.15	268.67	286.20	290.97	295.75	300.52	305.30
In each		C	288.10	296.57	305.00	313.52	322.00	328.72	335.45	342.17	348.90
Component	Tooth	a	60.18	93.08	125.98	158.88	191.80	210.50	229.20	247.90	266.60
		m	90.28	115.66	141.04	166.42	191.80	210.50	229.20	247.90	266.60
		c	120.40	144.20	168.00	191.80	215.63	228.37	241.11	253.85	266.60
		C	240.70	246.45	252.20	257.95	263.70	281.05	298.40	315.75	333.10
	Dentine	a	44.18	74.76	105.34	135.92	166.50	187.15	207.81	228.46	249.11
		m	44.18	74.76	105.34	135.92	166.50	187.15	207.81	228.46	249.11
		c	107.50	130.48	153.45	176.43	199.40	211.83	224.26	236.68	249.11
		C	54.28	57.66	61.04	64.41	67.79	69.88	71.97	74.06	76.15
	Bone	a	37.46	43.43	49.40	55.36	61.33	62.82	64.31	65.80	67.30
		m	37.46	38.32	39.17	40.02	40.89	43.27	45.67	48.00	50.47
		c	149.83	153.25	156.67	160.09	163.51	164.71	165.92	167.12	168.34
	NVB	NVB	1.71	1.92	2.14	2.35	2.56	3.01	3.45	3.90	4.34
	Pulp	a	0.15	0.17	0.19	0.20	0.22	0.26	0.30	0.33	0.37
		c	0.15	0.17	0.19	0.20	0.22	0.26	0.30	0.33	0.37
	PDL	a	3.00	3.49	3.98	4.46	4.96	5.78	6.62	7.43	8.25
		m	3.00	5.21	5.51	6.31	7.41	7.62	7.83	8.04	8.25
		c	5.22	6.68	8.15	9.61	11.07	12.91	14.75	16.58	18.43
Intrusion	Structure %		**100**	**100**	**100**	**100**	**100**	**100**	**100**	**100**	**100**
0.6 N/60 gf	Tooth + bracket %	a	**24.06**	**35.30**	**46.12**	**56.58**	**66.65**	**69.87**	**72.76**	**75.39**	**77.78**
Stress %		m	36.07	44.14	51.92	59.41	66.65	69.87	72.76	75.39	77.78
Reaching		c	72.18	76.59	80.83	84.93	88.88	85.68	82.79	80.17	77.78
Each		C	**96.23**	**97.22**	**98.17**	**99.11**	**100.00**	**96.80**	**93.90**	**91.28**	**88.89**

Table 3. *Cont.*

Resorption (mm)			**0**	**1**	**2**	**3**	**4**	**5**	**6**	**7**	**8**
Component	Tooth %	a	**20.10**	**30.51**	**40.55**	**50.22**	**59.57**	**61.98**	**64.16**	**66.13**	**67.92**
		m	30.15	37.92	45.39	52.61	59.57	61.98	64.16	66.13	67.92
		c	40.21	47.27	54.07	60.63	66.96	67.25	67.49	67.72	67.92
		C	**80.39**	**80.79**	**81.17**	**81.54**	**81.89**	**82.76**	**83.53**	**84.23**	**84.87**
	Dentine %	a	**14.76**	**24.51**	**33.90**	**42.97**	**51.71**	**55.11**	**58.17**	**60.94**	**63.47**
		m	14.76	24.51	33.90	42.97	51.71	55.11	58.17	60.94	63.47
		c	35.91	42.77	49.39	55.77	61.93	62.38	62.77	63.14	63.47
		C	**18.13**	**18.90**	**19.64**	**20.36**	**21.05**	**20.58**	**20.15**	**19.76**	**19.40**
	Bone %	a	**12.51**	**14.24**	**15.90**	**17.50**	**19.05**	**18.50**	**18.00**	**17.55**	**17.15**
		m	12.51	12.56	12.61	12.65	12.70	12.74	12.78	12.80	12.86
		c	**50.04**	**50.24**	**50.43**	**50.61**	**50.78**	**48.50**	**46.44**	**44.58**	**42.89**
	NVB %	NVB	**0.57**	**0.63**	**0.69**	**0.74**	**0.79**	**0.89**	**0.97**	**1.04**	**1.11**
	Pulp %	a	**0.05**	**0.05**	**0.06**	**0.06**	**0.07**	**0.08**	**0.08**	**0.09**	**0.09**
		c	**0.05**	**0.05**	**0.06**	**0.06**	**0.07**	**0.08**	**0.08**	**0.09**	**0.09**
	PDL %	a	**1.00**	**1.14**	**1.28**	**1.41**	**1.54**	**1.70**	**1.85**	**1.98**	**2.10**
		m	1.00	1.71	1.77	1.99	2.30	2.24	2.19	2.14	2.10
		c	**1.74**	**2.19**	**2.62**	**3.04**	**3.44**	**3.80**	**4.13**	**4.42**	**4.70**

structure—stress displayed by the 3D model. Tooth + bracket, Tooth, Dentine, Bone, NVB, Pulp, PDL components—stress displayed by these components. a—apical third, m—middle third, c—cervical third, C—crown. Tooth + bracket %, Tooth %, Dentine %, Bone %, NVB %, Pulp %, PDL % components—% stress displayed by these components.

3.3. Rotation (Figure 5, Table 4)

The highest quantitative stresses displayed among all five analyzed movements seem to be the most stressful movements. In intact periodontium, the stress around and on the bracket was 799.8 KPa, showing the same decreasing stress pattern (in tissular components) seen in extrusion and intrusion. In PDL cervical third, 0.6 N produced stresses under MHP. The dentine component displayed a high red-orange coronal stress under the bracket position. Stresses were concentrated in cervical third of radicular dentine, PDL, and alveolar socket bone. The quantitative amount of stress displayed by 1.2 N exceeded MHP only in cervical third of PDL, suggesting that it is safe to be clinically used (small neglectable areas of red-orange, Figure 5F). From a total of 799.8 KPa displayed at bracket level, only 8.98–21.19% are visible in radicular dentine, 9.6–38.37% in alveolar socket bone, 0.29–2.29% in PDL, 0.02–0.04% in pulp, and 0.22% in NVB.

In reduced periodontium, the displayed quantitative stresses at bracket level ranged between 803.35 and 890.4 KPa (for 0.6 N/approx. 60 gf), while only 16.96–77.69% reached radicular dentine, 10.54–45.19% alveolar bone socket, 0.38–7.67% PDL, 0.03–0.12% pulp, and 0.29–0.69% NVB. For radicular dentine component, a quantitative significant stress increase was visible during the periodontal breakdown (from 16–33.32% in 1 mm of loss to 58.35–77.69% in 8 mm of loss), while stress percentages for other components (alveolar bone socket, NVB, PDL, dental pulp) remained relatively constant. The radicular dentine displayed in the middle third qualitative red-orange areas of highly resorptive risks (especially in 8 mm of loss) correlated with bone loss. The coronal dentine stress decreases strictly correlated with bone loss. PDL cervical third stress (for 0.6 N) displayed qualitative red-orange areas which are more prone to further loss and quantitative values exceeding MHP (4 times for 8 mm of loss). Based on the above, 0.6 N can be safely applied in both intact and reduced periodontium, with the observation that PDL cervical third could suffer from ischemia and further loss. Rotational movement displayed increased stress in the entire alveolar bone socket (i.e., especially the cervical third, 40.18–45.19% of bracket stress) and correlated with periodontal breakdown. During the rotational movement in both intact and reduced periodontium, only the dentine component displayed significant red-orange high stress areas.

The 1.2 N force produced similar qualitative results as 0.6 N, and quantitative higher amounts of stress (doubling the numerical values when compared with 0.6 N), being prone

to ischemic and resorptive risks in both middle and cervical third PDL and radicular dentine.

The bracket absorption–dissipation ability was 18.73% in 0 mm, 17.63% in 1 mm, and 17.48% in 8 mm loss.

The enamel absorption–dissipation ability was 60.09% in 0 mm, 60.09% in 1 mm, and 62.84% in 8 mm loss.

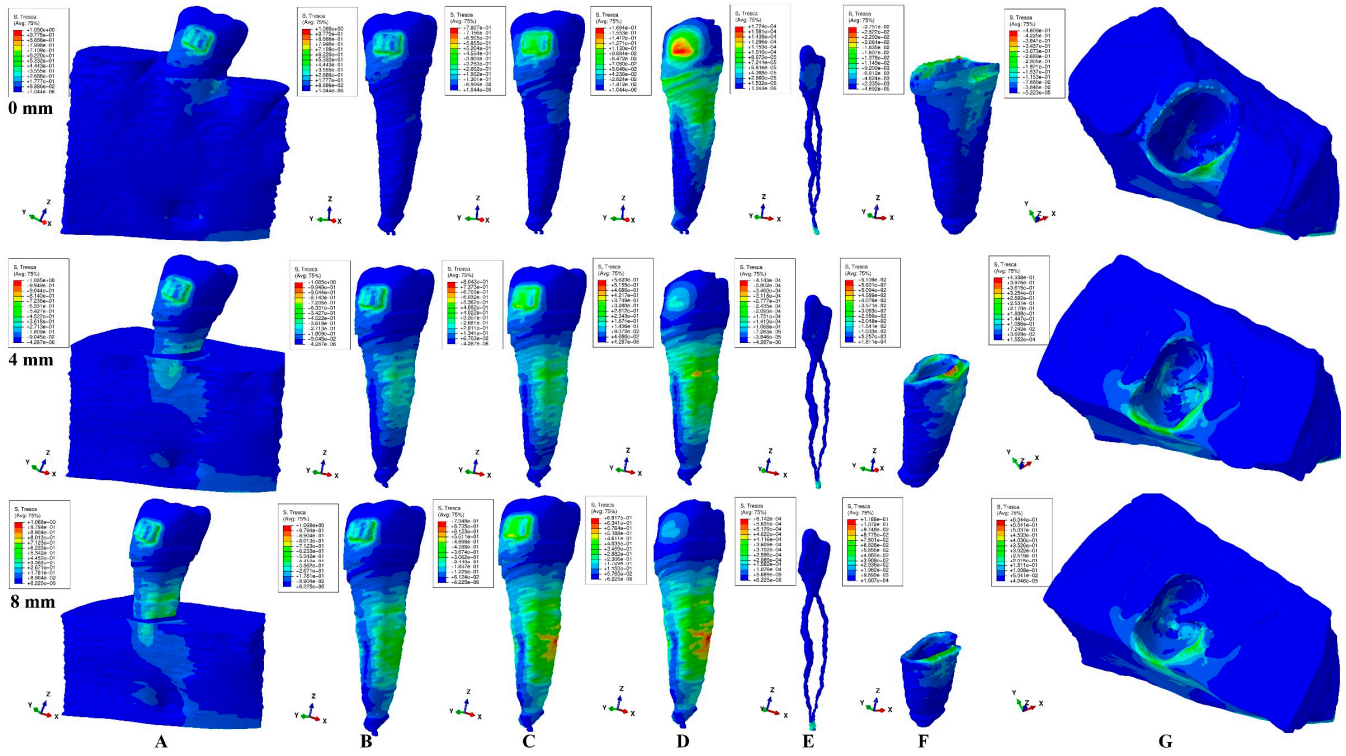

Figure 5. Rotation—Tresca stress display in dental tissues subjected to 0.6 N for 0, 4, and 8 mm bone loss: (**A**)—dental tissues' structure, (**B**)—tooth with bracket, (**C**)—tooth without bracket, (**D**)—dentine component, (**E**)—dental pulp and NVB, (**F**)—PDL, (**G**)—bone with alveolar socket.

Table 4. Maximum stress average values (KPa) produced by orthodontic forces in tooth structure and dentine–cementum.

Resorption (mm)			**0**	**1**	**2**	**3**	**4**	**5**	**6**	**7**	**8**
Rotation	Structure		**799.80**	**803.35**	**806.90**	**810.45**	**814.00**	**833.10**	**852.20**	**871.30**	**890.40**
0.6 N/60 gf	Tooth + bracket	a	88.60	156.90	225.20	293.50	361.80	427.17	492.54	557.91	623.30
Stress		m	88.60	224.70	360.84	496.96	633.10	675.15	717.20	759.25	801.30
Amount		c	177.70	291.55	405.40	519.25	633.10	652.90	672.70	692.50	712.30
In each		C	799.80	803.35	806.90	810.45	814.00	833.10	852.20	871.30	890.40
Component	Tooth	a	81.00	144.52	208.00	271.56	335.10	389.20	443.30	497.40	551.50
		m	81.00	178.00	275.10	372.15	469.20	535.60	602.00	668.40	734.80
		c	195.20	297.20	399.30	501.20	603.20	605.47	607.75	610.02	612.30
		C	650.00	657.32	664.65	671.97	679.30	693.17	707.05	720.92	734.80
	Dentine	a	71.84	136.25	200.66	265.07	329.48	376.99	424.50	472.01	519.52
		m	71.84	159.55	247.27	334.99	422.70	489.96	557.21	624.47	691.72
		c	169.46	267.67	365.89	464.10	562.31	565.96	569.62	573.27	576.92
		C	169.43	174.34	179.24	184.15	189.65	186.04	182.42	178.81	175.19
	Bone	a	76.74	84.65	92.57	100.48	108.39	119.02	129.64	140.26	150.88
		m	76.74	84.65	92.57	100.48	108.39	119.02	129.64	140.26	150.88
		c	306.88	322.78	338.66	354.55	370.45	378.43	386.42	394.42	402.41

Table 4. *Cont.*

Resorption (mm)			**0**	**1**	**2**	**3**	**4**	**5**	**6**	**7**	**8**
	NVB	NVB	1.72	2.33	2.93	3.54	4.14	4.64	5.14	5.64	6.14
	Pulp	a	0.15	0.21	0.27	0.33	0.38	0.43	0.48	0.52	0.57
		c	0.29	0.43	0.51	0.62	0.73	0.82	0.91	0.99	1.08
	PDL	a	2.34	3.07	3.80	4.53	5.26	6.42	7.58	8.73	9.89
		m	4.62	6.05	7.48	8.90	10.33	12.65	14.98	17.30	19.62
		c	18.35	25.23	32.11	38.98	45.86	51.47	57.07	62.68	68.28
Rotation	Structure %		**100**	**100**	**100**	**100**	**100**	**100**	**100**	**100**	**100**
0.6 N/60 gf	Tooth + bracket %	a	**11.08**	**19.53**	**27.91**	**36.21**	**44.45**	**51.27**	**57.80**	**64.03**	**70.00**
Stress %		m	11.08	27.97	44.72	61.32	77.78	81.04	84.16	87.14	89.99
Reaching		c	22.22	36.29	50.24	64.07	77.78	78.37	78.94	79.48	80.00
Each		C	**100.00**	**100.00**	**100.00**	**100.00**	**100.00**	**100.00**	**100.00**	**100.00**	**100.00**
Component	Tooth %	a	**10.13**	**17.99**	**25.78**	**33.51**	**41.17**	**46.72**	**52.02**	**57.09**	**61.94**
		m	10.13	22.16	34.09	45.92	57.64	64.29	70.64	76.71	82.52
		c	24.41	37.00	49.49	61.84	74.10	72.68	71.32	70.01	68.77
		C	**81.27**	**81.82**	**82.37**	**82.91**	**83.45**	**83.20**	**82.97**	**82.74**	**82.52**
	Dentine %	a	**8.98**	**16.96**	**24.87**	**32.71**	**40.48**	**45.25**	**49.81**	**54.17**	**58.35**
		m	8.98	19.86	30.64	41.33	51.93	58.81	65.38	71.67	77.69
		c	21.19	33.32	45.34	57.26	69.08	67.93	66.84	65.79	64.79
		C	**21.18**	**21.70**	**22.21**	**22.72**	**23.30**	**22.33**	**21.41**	**20.52**	**19.68**
	Bone %	a	**9.60**	**10.54**	**11.47**	**12.40**	**13.32**	**14.29**	**15.21**	**16.10**	**16.95**
		m	9.60	10.54	11.47	12.40	13.32	14.29	15.21	16.10	16.95
		c	**38.37**	**40.18**	**41.97**	**43.75**	**45.51**	**45.42**	**45.34**	**45.27**	**45.19**
	NVB %	NVB	**0.22**	**0.29**	**0.36**	**0.44**	**0.51**	**0.56**	**0.60**	**0.65**	**0.69**
	Pulp %	a	**0.02**	**0.03**	**0.03**	**0.04**	**0.05**	**0.05**	**0.06**	**0.06**	**0.06**
		c	**0.04**	**0.05**	**0.06**	**0.08**	**0.09**	**0.10**	**0.11**	**0.11**	**0.12**
	PDL %	a	**0.29**	**0.38**	**0.47**	**0.56**	**0.65**	**0.77**	**0.89**	**1.00**	**1.11**
		m	0.58	0.75	0.93	1.10	1.27	1.52	1.76	1.99	2.20
		c	**2.29**	**3.14**	**3.98**	**4.81**	**5.63**	**6.18**	**6.70**	**7.19**	**7.67**

structure—stress displayed by the 3D model. Tooth + bracket, Tooth, Dentine, Bone, NVB, Pulp, PDL components—stress displayed by these components. a—apical third, m—middle third, c—cervical third, C—crown. Tooth + bracket %, Tooth %, Dentine %, Bone %, NVB %, Pulp %, PDL % components—% stress displayed by these components.

3.4. Translation (Figure 6, Table 5)

Based on quantitative and qualitative results, translation seems to be the second most stressful movement after rotation. In intact periodontium, translation displayed 504.4 KPa at bracket level, with visible stresses in cervical third of radicular dentine, PDL, and alveolar bone socket. Translation is the single movement that displayed a clearly visible stress in coronal pulp. From the 504.4 KPa displayed at bracket level, 13.47–39.67% reaches radicular dentine, 14–36.73% alveolar bone socket, 0.02–0.06% pulp, 0.4–3.51% PDL, and 0.22% NVB.

In reduced periodontium, the increase in quantitative stress results correlated with bone loss. Qualitatively, stress areas extended in the entire radicular dentine with red-orange areas displayed in middle and apical third, being prone to external resorptive and ischemic processes. Quantitively, a visible increase in stress amount during periodontal breakdown was clearly visible in the radicular dentine component ranging from 15.57–49.57% in 1 mm loss up to 62–92.9% in 8 mm loss (more pronounced in radicular middle third after 4 mm bone loss). The absorption–dissipation ability of the other tissular components remained constant, 16.98–41.57% in alveolar bone socket, 0.51–8.37% PDL, 0.02–0.08% pulp, and 0.25–0.32% in NVB during the bone loss process when compared with the other movements. The qualitative coronal pulp stress display remained visible during bone loss, but with a clearly decreasing pattern. Moreover, the qualitative alveolar bone socket stress display showed a decreasing stress pattern.

In both intact and reduced periodontium, 0.6 N seems to be safe for application (only PDL cervical third stress exceeded MHP). Both 0.6 N and 1.2 N showed similar qualitative stress display areas, with a doubling of quantitative results for 1.2 N. PDL displayed stresses exceeding physiological MHP during bone loss simulations, in both middle and cervical

third (especially after 4 mm of loss, visible red-orange high stress areas), which seem to be prone to ischemic and resorptive processes.

The bracket absorption–dissipation ability was 29.04% in 0 mm, 28.79% in 1 mm, and 45.81% in 8 mm loss.

The enamel absorption–dissipation ability was 57.49% in 0 mm, 57.44% in 1 mm, and 38.53% in 8 mm loss.

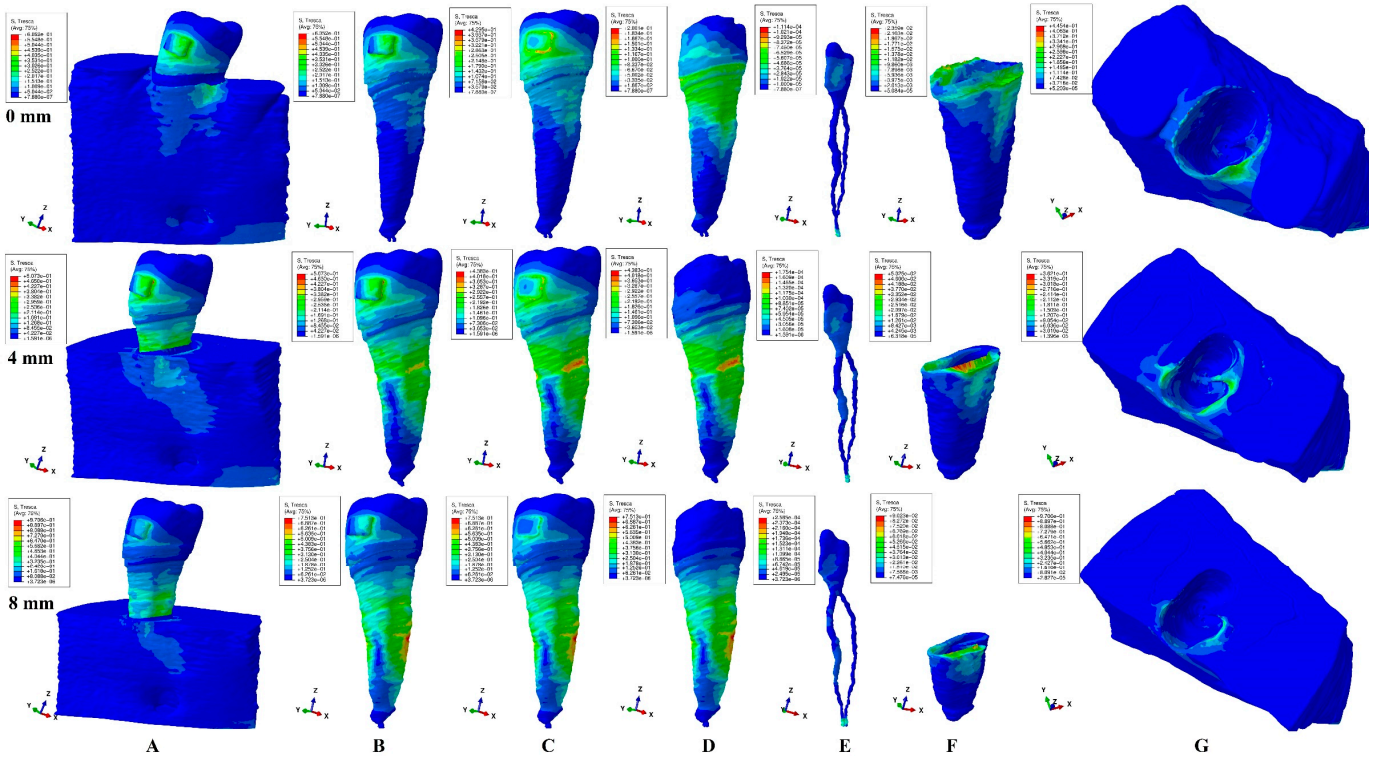

Figure 6. Translation—Tresca stress display in dental tissues subjected to 0.6 N for 0, 4, and 8 mm bone loss: (**A**)—dental tissues' structure, (**B**)—tooth with bracket, (**C**)—tooth without bracket, (**D**)—dentine component, (**E**)—dental pulp and NVB, (**F**)—PDL, (**G**)—bone with alveolar socket.

Table 5. Maximum stress average values (KPa) produced by orthodontic forces in tooth structure and dentine–cementum.

Resorption (mm)			**0**	**1**	**2**	**3**	**4**	**5**	**6**	**7**	**8**
Translation	Structure		**504.40**	**505.10**	**505.80**	**506.50**	**507.30**	**582.67**	**658.00**	**733.40**	**808.80**
0.6 N/60 gf	Tooth + bracket	a	100.90	117.95	135.00	152.05	169.10	267.70	366.30	464.90	563.61
Stress		m	100.90	191.92	282.90	373.90	465.00	536.58	608.10	679.70	751.35
Amount		c	202.41	268.00	333.69	399.30	465.00	489.60	415.30	538.90	563.61
In each		C	504.40	505.10	505.80	506.50	507.30	582.67	658.00	733.40	808.80
Component	Tooth	a	71.50	90.10	108.80	127.40	146.10	250.47	354.84	459.20	563.61
		m	71.50	163.20	254.90	346.60	438.31	516.50	594.80	673.00	751.35
		c	202.41	261.37	320.34	379.30	438.31	469.60	500.90	532.20	563.61
		C	357.90	359.70	361.60	363.40	365.30	383.55	401.80	420.00	438.30
	Dentine	a	67.94	78.67	89.40	100.12	110.85	208.50	306.16	403.81	501.46
		m	67.94	160.53	253.13	345.72	438.31	516.57	594.83	673.09	751.35
		c	200.11	250.38	300.65	350.91	401.18	441.88	482.57	523.27	563.96
		C	67.94	69.55	71.16	72.77	74.38	87.45	100.51	113.58	126.64
	Bone	a	74.17	85.75	97.33	108.92	120.51	130.76	141.04	151.30	161.57
		m	74.17	85.75	97.33	108.92	120.51	130.76	141.04	151.30	161.57
		c	185.28	191.68	198.08	204.49	210.90	220.91	230.93	240.95	250.97

Table 5. *Cont.*

Resorption (mm)			**0**	**1**	**2**	**3**	**4**	**5**	**6**	**7**	**8**
	NVB	NVB	1.11	1.27	1.43	1.59	1.75	1.97	2.18	2.38	2.59
	Pulp	a	0.11	0.12	0.13	0.15	0.16	0.18	0.21	0.23	0.25
		c	0.28	0.32	0.37	0.41	0.45	0.51	0.56	0.62	0.67
	PDL	a	2.01	2.57	3.13	3.69	4.25	5.06	5.88	6.69	7.51
		m	3.97	5.09	6.20	7.31	8.43	10.09	11.76	13.43	15.10
		c	17.71	23.76	29.80	35.84	41.89	48.29	54.69	61.10	67.70
Translation	Structure %		**100**	**100**	**100**	**100**	**100**	**100**	**100**	**100**	**100**
0.6 N/60 gf	Tooth + bracket %	a	**20.00**	**23.35**	**26.69**	**30.02**	**33.33**	**45.94**	**55.67**	**63.39**	**69.68**
Stress %		m	20.00	38.00	55.93	73.82	91.66	92.09	92.42	92.68	92.90
Reaching		c	40.13	53.06	65.97	78.84	91.66	84.03	63.12	73.48	69.68
Each		C	**100.00**	**100.00**	**100.00**	**100.00**	**100.00**	**100.00**	**100.00**	**100.00**	**100.00**
Component	Tooth %	a	**14.18**	**17.84**	**21.51**	**25.15**	**28.80**	**42.99**	**53.93**	**62.61**	**69.68**
		m	14.18	32.31	50.40	68.43	86.40	88.64	90.40	91.76	92.90
		c	40.13	51.75	63.33	74.89	86.40	80.59	76.12	72.57	69.68
		C	**70.96**	**71.21**	**71.49**	**71.75**	**72.01**	**65.83**	**61.06**	**57.27**	**54.19**
	Dentine %	a	**13.47**	**15.57**	**17.67**	**19.77**	**21.85**	**35.78**	**46.53**	**55.06**	**62.00**
		m	13.47	31.78	50.04	68.26	86.40	88.66	90.40	91.78	92.90
		c	39.67	49.57	59.44	69.28	79.08	75.84	73.34	71.35	69.73
		C	**13.47**	**13.77**	**14.07**	**14.37**	**14.66**	**15.01**	**15.28**	**15.49**	**15.66**
	Bone %	a	**14.70**	**16.98**	**19.24**	**21.50**	**23.75**	**22.44**	**21.43**	**20.63**	**19.98**
		m	14.70	16.98	19.24	21.50	23.75	22.44	21.43	20.63	19.98
		c	**36.73**	**37.95**	**39.16**	**40.37**	**41.57**	**37.91**	**35.10**	**32.85**	**31.03**
	NVB %	NVB	**0.22**	**0.25**	**0.28**	**0.31**	**0.35**	**0.34**	**0.33**	**0.32**	**0.32**
	Pulp %	a	**0.02**	**0.02**	**0.03**	**0.03**	**0.03**	**0.03**	**0.03**	**0.03**	**0.03**
		c	**0.06**	**0.06**	**0.07**	**0.08**	**0.09**	**0.09**	**0.09**	**0.08**	**0.08**
	PDL %	a	**0.40**	**0.51**	**0.62**	**0.73**	**0.84**	**0.87**	**0.89**	**0.91**	**0.93**
		m	0.79	1.01	1.23	1.44	1.66	1.73	1.79	1.83	1.87
		c	**3.51**	**4.70**	**5.89**	**7.08**	**8.26**	**8.29**	**8.31**	**8.33**	**8.37**

structure—stress displayed by the 3D model. Tooth + bracket, Tooth, Dentine, Bone, NVB, Pulp, PDL components—stress displayed by these components. a—apical third, m—middle third, c—cervical third, C—crown. Tooth + bracket %, Tooth %, Dentine %, Bone %, NVB %, Pulp %, PDL % components—% stress displayed by these components.

3.5. Tipping (Figure 7, Table 6)

In intact periodontium, the maximum amount of stress displayed at bracket level was 366.1 KPa, which is closer to the intrusion and extrusion movements, whereas the qualitative stress was concentrated in cervical third of radicular dentine and PDL. Of the total amount of stress, only 16.39–32.4% reached radicular dentine, 20–40% alveolar bone socket, 0.42–3.31% PDL, 0.03–0.04% pulp, and 0.4% NVB. All quantitative stresses displayed in PDL, dental pulp, and NVB were lower than MHP.

Reduced periodontium displayed an extension of high stress areas (i.e., red-orange) in the entire radicular dentine and PDL cervical third, signaling potential areas of ischemic and resorptive risks. The stress increases in bone alveolar socket correlated with bone loss. Quantitatively, the circulatory sensitive tissues (PDL, NVB, and dental pulp) for both 0.6 and 1.2 N amounts of stress were lower than MHP (except in cervical third after 2–5 mm of loss), which seem to be safe for application up to 8 mm of bone loss (Figure 8 and Table 7). The radicular dentine component showed a quantitatively increasing stress pattern ranging from 23.4–40.68% in 1 mm loss to 70.94–85% in 8 mm loss, which is correlated with the bone loss process and qualitatively visible (red-orange areas are prone to resorptive processes). Of the total amount of stress of 380.4–544.1 KPa, only 20.63–44.46% reached alveolar bone socket, 0.62–8.25% PDL, 0.04–0.07% pulp, and 0.48–0.82% NVB.

The bracket absorption–dissipation ability was 16.69% in 0 mm, 18.16% in 1 mm, and 16.35% in 8 mm loss.

The enamel absorption–dissipation ability was 50.29% in 0 mm, 49.09% in 1 mm, and 42.31% in 8 mm loss.

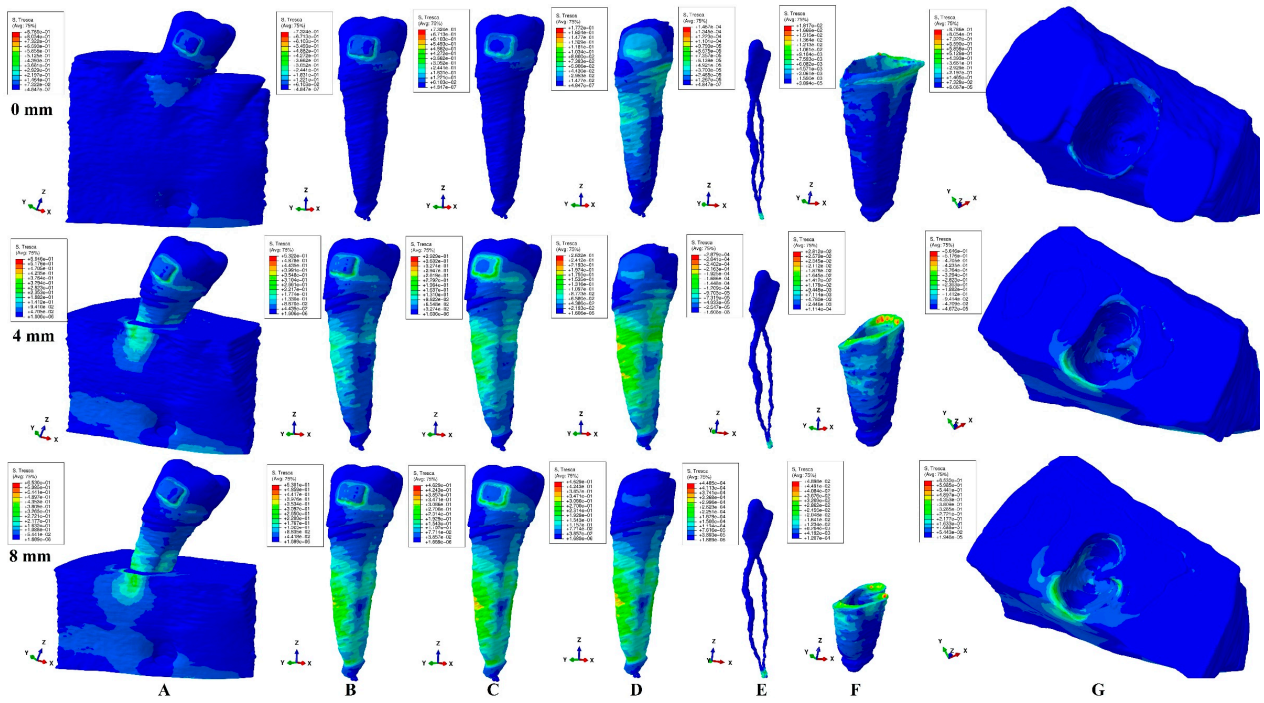

Figure 7. Tipping—Tresca stress display in dental tissues subjected to 0.6 N for 0, 4, and 8 mm bone loss: (**A**)—dental tissues' structure, (**B**)—tooth with bracket, (**C**)—tooth without bracket, (**D**)—dentine component, (**E**)—dental pulp and NVB, (**F**)—PDL, (**G**)—bone with alveolar socket.

Table 6. Maximum stress average values (KPa) produced by orthodontic forces in tooth structure and dentine–cementum.

Resorption (mm)			**0**	**1**	**2**	**3**	**4**	**5**	**6**	**7**	**8**
Tipping	Structure		**366.10**	**380.40**	**394.80**	**409.15**	**423.50**	**453.60**	**483.80**	**513.90**	**544.10**
0.6 N/60 gf	Tooth + bracket	a	61.67	112.85	164.03	215.20	266.41	299.20	331.90	364.70	397.60
Stress		m	61.67	134.95	208.20	281.50	354.80	387.50	420.30	453.10	485.90
Amount		c	122.61	180.60	238.70	296.70	354.80	365.50	376.20	386.90	397.60
In each		C	305.20	317.60	330.00	342.50	354.80	365.50	376.20	386.20	397.60
Component	Tooth	a	61.67	96.35	128.00	162.70	196.40	243.70	291.00	338.36	385.70
		m	61.67	119.90	178.10	236.40	294.70	336.75	378.80	420.80	462.92
		c	122.61	165.60	208.60	251.60	294.70	317.40	340.20	362.90	385.70
		C	244.10	248.50	253.00	257.40	261.90	273.50	285.20	296.90	308.60
	Dentine	a	60.01	89.00	118.00	147.00	176.00	228.50	281.00	333.50	386.00
		m	60.01	99.92	139.84	179.75	219.66	280.48	341.29	402.11	462.92
		c	118.61	154.76	190.91	227.06	263.21	293.91	324.61	355.30	386.00
		C	60.01	61.76	63.51	65.26	67.01	69.85	72.70	75.54	78.38
	Bone	a	73.27	78.48	83.70	88.92	94.14	97.81	101.50	105.17	108.85
		m	73.27	78.48	83.70	88.92	94.14	97.81	101.50	105.17	108.85
		c	146.53	156.97	167.41	177.85	188.29	195.64	202.99	210.34	217.69
	NVB	NVB	1.47	1.82	2.18	2.53	2.88	3.28	3.69	4.09	4.49
	Pulp	a	0.13	0.17	0.19	0.23	0.25	0.29	0.33	0.36	0.39
		c	0.15	0.18	0.21	0.23	0.25	0.29	0.33	0.36	0.39
	PDL	a	1.55	2.36	3.16	3.96	4.78	5.65	6.52	7.39	8.26
		m	3.06	4.07	5.09	6.10	7.11	8.42	9.73	11.03	12.34
		c	12.13	15.55	18.96	22.38	25.79	30.57	35.35	40.13	44.91
Tipping	Structure %		**100**	**100**	**100**	**100**	**100**	**100**	**100**	**100**	**100**
0.6 N/60 gf	Tooth + bracket %	a	**16.84**	**29.67**	**41.55**	**52.60**	**62.91**	**65.96**	**68.60**	**70.97**	**73.07**
Stress %		m	16.84	35.48	52.74	68.80	83.78	85.43	86.87	88.17	89.30
Reaching		c	33.49	47.48	60.46	72.52	83.78	80.58	77.76	75.29	73.07
Each		C	**83.37**	**83.49**	**83.59**	**83.71**	**83.78**	**80.58**	**77.76**	**75.15**	**73.07**
Component	Tooth %	a	**16.84**	**25.33**	**32.42**	**39.77**	**46.38**	**53.73**	**60.15**	**65.84**	**70.89**
		m	16.84	31.52	45.11	57.78	69.59	74.24	78.30	81.88	85.08
		c	33.49	43.53	52.84	61.49	69.59	69.97	70.32	70.62	70.89

Table 6. *Cont.*

Resorption (mm)		0	1	2	3	4	5	6	7	8
Dentine %	C	**66.68**	**65.33**	**64.08**	**62.91**	**61.84**	**60.30**	**58.95**	**57.77**	**56.72**
	a	**16.39**	**23.40**	**29.89**	**35.93**	**41.56**	**50.37**	**58.08**	**64.90**	**70.94**
	m	16.39	26.27	35.42	43.93	51.87	61.83	70.54	78.25	85.08
	c	32.40	40.68	48.36	55.50	62.15	64.79	67.09	69.14	70.94
Bone %	C	**16.39**	**16.24**	**16.09**	**15.95**	**15.82**	**15.40**	**15.03**	**14.70**	**14.41**
	a	**20.01**	**20.63**	**21.20**	**21.73**	**22.23**	**21.56**	**20.98**	**20.46**	**20.01**
	m	20.01	20.63	21.20	21.73	22.23	21.56	20.98	20.46	20.01
	c	**40.02**	**41.26**	**42.40**	**43.47**	**44.46**	**43.13**	**41.96**	**40.93**	**40.01**
NVB %	NVB	**0.40**	**0.48**	**0.55**	**0.62**	**0.68**	**0.72**	**0.76**	**0.80**	**0.82**
Pulp %	a	**0.03**	**0.04**	**0.05**	**0.06**	**0.06**	**0.06**	**0.07**	**0.07**	**0.07**
	c	**0.04**	**0.05**	**0.05**	**0.06**	**0.06**	**0.06**	**0.07**	**0.07**	**0.07**
PDL %	a	**0.42**	**0.62**	**0.80**	**0.97**	**1.13**	**1.25**	**1.35**	**1.44**	**1.52**
	m	0.84	1.07	1.29	1.49	1.68	1.86	2.01	2.15	2.27
	c	**3.31**	**4.09**	**4.80**	**5.47**	**6.09**	**6.74**	**7.31**	**7.81**	**8.25**

structure—stress displayed by the 3D model. Tooth + bracket, Tooth, Dentine, Bone, NVB, Pulp, PDL components—stress displayed by these components. a—apical third, m—middle third, c—cervical third, C—crown. Tooth + bracket %, Tooth %, Dentine %, Bone %, NVB %, Pulp %, PDL % components—% stress displayed by these components.

In intact periodontium, both forces (0.6 and 1.2 N) seem to be safe for application (lower than MHP). Nevertheless, in reduced periodontium, 0.6 N of the applied force produced a cervical third PDL stress that is higher than physiological MHP (i.e., after 2–5 mm of loss, with higher resorptive risks). A force of 2.4 N exceeded the physiological MHP for all movements and bone levels, thus ischemic and resorptive risks are the highest (Figure 8 and Table 7). Nevertheless, the stress absorption–dissipation pattern displayed by the other two lower loads remained constant.

As biomechanically expected in all movements and bone loss levels, the radicular dentine component showed variable quantitative and qualitative stress displays (% of total stress reaching the dentine component, Figures 3–7, Tables 2–6), while all other tissular components showed a relatively constant %, emphasizing dentine and enamel components' primary role in the absorption–dissipation ability of dental structures.

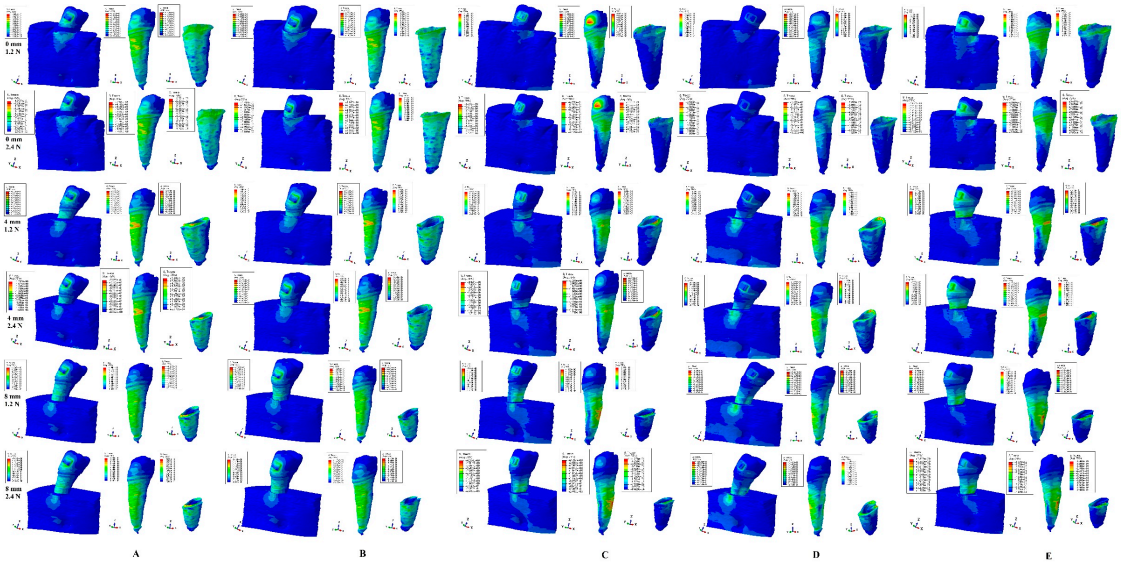

Figure 8. Comparative qualitative and quantitative results for 1.2 and 2.4 N forces for 0, 4, and 8 mm bone loss for dental tissues' structure, dentine, and PDL components: (**A**)—extrusion, (**B**)—intrusion, (**C**)—rotation, (**D**)—tipping, (**E**)—translation.

Table 7. Maximum stress average values (KPa) produced by orthodontic forces in tooth structure, dentine–cementum, and PDL.

Resorption (mm)			**0**	**1**	**2**	**3**	**4**	**5**	**6**	**7**	**8**
Extrusion	Structure		598.8	610.1	621.4	632.7	644	679.2	714.5	749.74	785
1.2 N/ 120 gf	Dentine	a	88.35	149.52	210.68	271.84	333.00	374.31	415.61	456.92	498.22
		m	88.35	149.52	210.68	271.84	333.00	374.31	415.61	456.92	498.22
		c	215.00	260.95	306.90	352.85	398.80	423.66	448.51	473.37	498.22
		C	108.56	115.32	122.07	128.83	135.57	139.76	143.94	148.12	152.30
PDL Stress	**PDL**	a	5.99	7.59	9.18	10.77	12.37	13.40	14.43	15.47	16.50
Exceeding		m	5.99	7.59	9.18	10.77	12.37	13.40	14.43	15.47	16.50
MHP		**c**	**13.41**	**16.81**	**20.22**	**23.63**	**27.04**	**31.54**	**36.07**	**40.59**	**45.10**
2.4 N/ 240 gf	Structure		1197.6	1220.2	1242.8	1265.4	1288	1358.4	1429	1499.48	1570
	Dentine	a	176.71	299.04	421.36	543.68	666.00	748.61	831.22	913.83	996.43
		m	176.71	299.04	421.36	543.68	666.00	748.61	831.22	913.83	996.43
		c	430.00	521.90	613.80	705.70	797.60	847.31	897.02	946.73	996.43
		C	217.12	230.63	244.14	257.65	271.14	279.52	287.88	296.24	304.60
PDL Stress	**PDL**	**a**	11.99	15.18	18.36	**21.54**	**24.73**	**26.79**	**28.86**	**30.93**	**33.00**
Exceeding		**m**	11.99	15.18	18.36	**21.54**	**24.73**	**26.79**	**28.86**	**30.93**	**33.00**
MHP		**c**	**26.82**	**33.62**	**40.44**	**47.26**	**54.08**	**63.08**	**72.14**	**81.17**	**90.20**
Intrusion	Structure		598.8	610.1	621.4	632.7	644	679.2	714.5	749.74	785
1.2 N/ 120 gf	Dentine	a	88.35	149.52	210.68	271.84	333.00	374.31	415.61	456.92	498.22
		m	88.35	149.52	210.68	271.84	333.00	374.31	415.61	456.92	498.22
		c	215.00	260.95	306.90	352.85	398.80	423.66	448.51	473.37	498.22
		C	108.56	115.32	122.07	128.83	135.57	139.76	143.94	148.12	152.30
PDL Stress	**PDL**	a	5.99	6.98	7.95	8.93	9.92	11.55	13.23	14.85	16.50
Exceeding		m	5.99	10.41	11.01	12.62	14.81	15.24	15.66	16.08	16.50
MHP		**c**	10.44	13.37	16.30	**19.22**	**22.15**	**25.82**	**29.49**	**33.17**	**36.86**
2.4 N/ 240 gf	Structure		1197.6	1220.2	1242.8	1265.4	1288	1358.4	1429	1499.48	1570
	Dentine	a	176.71	299.04	421.36	543.68	666.00	748.61	831.22	913.83	996.43
		m	176.71	299.04	421.36	543.68	666.00	748.61	831.22	913.83	996.43
		c	430.00	521.90	613.80	705.70	797.60	847.31	897.02	946.73	996.43
		C	217.12	230.63	244.14	257.65	271.14	279.52	287.88	296.24	304.60
PDL Stress	**PDL**	**a**	11.99	13.95	15.90	**17.85**	**19.84**	**23.10**	**26.46**	**29.70**	**33.00**
Exceeding		**m**	11.99	**20.83**	**22.02**	**25.23**	**29.62**	**30.48**	**31.32**	**32.16**	**33.00**
MHP		**c**	**20.88**	**26.73**	**32.59**	**38.43**	**44.29**	**51.63**	**58.99**	**66.33**	**73.71**
Rotation	Structure		1599.60	1606.70	1613.80	1620.90	1628.00	1666.20	1704.40	1742.60	1780.80
1.2 N/ 120 gf	Dentine	a	143.67	272.50	401.32	530.14	658.95	753.98	849.00	944.02	1039.04
		m	143.67	319.10	494.54	669.97	845.40	979.91	1114.42	1248.93	1383.44
		c	338.91	535.35	731.77	928.20	1124.63	1131.93	1139.23	1146.54	1153.84
		C	338.86	348.67	358.48	368.29	379.30	372.07	364.84	357.61	350.37
PDL Stress	PDL	**a**	4.67	6.14	7.60	9.06	10.51	12.83	15.15	**17.47**	**19.79**
Exceeding		**m**	9.25	12.10	14.95	**17.81**	**20.67**	**25.31**	**29.95**	**34.60**	**39.24**
MHP		**c**	**36.70**	**50.46**	**64.21**	**77.97**	**91.72**	**102.93**	**114.14**	**125.35**	**136.56**
2.4 N/ 240 gf	Structure		3199.20	3213.40	3227.60	3241.80	3256.00	3332.40	3408.80	3485.20	3561.60
	Dentine	a	287.34	545.00	802.64	1060.28	1317.90	1507.96	1698.00	1888.04	2078.07
		m	287.34	638.20	989.08	1339.94	1690.79	1959.82	2228.84	2497.86	2766.87
		c	677.82	1070.69	1463.54	1856.39	2249.26	2263.85	2278.46	2293.07	2307.67
		C	677.72	697.34	716.96	736.58	758.60	744.14	729.68	715.22	700.75
PDL Stress	**PDL**	**a**	9.34	12.29	15.21	**18.13**	**21.03**	**25.67**	**30.30**	**34.93**	**39.57**
Exceeding		**m**	**18.50**	**24.19**	**29.90**	**35.61**	**41.34**	**50.61**	**59.90**	**69.19**	**78.48**
MHP		**c**	**73.41**	**100.91**	**128.42**	**155.93**	**183.44**	**205.86**	**228.29**	**250.70**	**273.12**
Translation	Structure		1008.80	1010.20	1011.60	1013.00	1014.60	1165.34	1316.00	1466.80	1617.60
1.2 N/ 120 gf	Dentine	a	135.88	157.34	178.79	200.25	221.69	417.01	612.31	807.62	1002.92
		m	135.88	321.07	506.25	691.44	876.62	1033.14	1189.66	1346.18	1502.69
		c	400.21	500.76	601.29	701.83	802.36	883.75	965.14	1046.53	1127.93
		C	135.88	139.10	142.32	145.54	148.76	174.89	201.02	227.15	253.28

Table 7. *Cont.*

Resorption (mm)			0	1	2	3	4	5	6	7	8
PDL Stress Exceeding MHP	**PDL**	a	4.03	5.15	6.26	7.38	8.49	10.13	11.75	13.39	15.02
		m	7.95	10.18	12.40	14.63	16.85	**20.19**	**23.53**	**26.86**	**30.20**
		c	**35.43**	**47.52**	**59.60**	**71.69**	**83.77**	**96.58**	**109.39**	**122.19**	**135.40**
2.4 N/ 240 gf	Structure		2017.60	2020.40	2023.20	2026.00	2029.20	2330.68	2632.00	2933.60	3235.20
	Dentine	a	271.76	314.67	357.58	400.49	443.39	834.01	1224.62	1615.23	2005.84
		m	271.76	642.13	1012.50	1382.87	1753.25	2066.28	2379.32	2692.36	3005.39
		c	800.43	1001.51	1202.58	1403.65	1604.72	1767.50	1930.28	2093.06	2255.86
		C	271.76	278.20	284.64	291.08	297.52	349.78	402.04	454.30	506.56
PDL Stress Exceeding MHP	**PDL**	**a**	8.05	10.29	12.52	14.75	16.98	**20.26**	**23.50**	**26.78**	**30.05**
		m	15.90	**20.35**	**24.80**	**29.25**	**33.70**	**40.38**	**47.05**	**53.73**	**60.40**
		c	**70.86**	**95.03**	**119.20**	**143.37**	**167.54**	**193.16**	**218.77**	**244.39**	**270.80**
Tipping 1.2 N/ 120 gf	Structure		732.20	760.80	789.60	818.30	847.00	907.20	967.60	1027.80	1088.20
	Dentine	a	120.03	178.00	236.00	294.00	352.00	457.00	562.00	667.00	772.00
		m	120.03	199.85	279.67	359.50	439.33	560.95	682.58	804.21	925.83
		c	237.21	309.52	381.82	454.12	526.42	587.82	649.21	710.61	772.00
		C	120.03	123.52	127.02	130.52	134.02	139.71	145.39	151.08	156.77
PDL Stress Exceeding MHP	**PDL**	a	3.10	4.72	6.32	7.92	9.56	11.30	13.04	14.78	**16.53**
		m	6.12	8.15	10.17	12.20	14.22	16.84	**19.45**	**22.07**	**24.68**
		c	**24.26**	**31.09**	**37.92**	**44.75**	**51.58**	**61.14**	**70.70**	**80.26**	**89.82**
2.4 N/ 240 gf	Structure		1464.40	1521.60	1579.20	1636.60	1694.00	1814.40	1935.20	2055.60	2176.40
	Dentine	a	240.06	356.00	472.00	588.00	704.01	914.00	1124.00	1334.00	1544.00
		m	240.06	399.69	559.34	718.99	878.66	1121.90	1365.16	1608.42	1851.66
		c	474.43	619.04	763.64	908.24	1052.84	1175.63	1298.42	1421.21	1544.00
		C	240.06	247.04	254.04	261.04	268.05	279.41	290.78	302.15	313.54
PDL Stress Exceeding MHP	**PDL**	**a**	6.20	9.43	12.63	15.83	**19.12**	**22.60**	**26.08**	**29.56**	**33.06**
		m	12.24	16.29	**20.34**	**24.39**	**28.44**	**33.67**	**38.90**	**44.13**	**49.36**
		c	**48.52**	**62.18**	**75.84**	**89.50**	**103.16**	**122.28**	**141.40**	**160.52**	**179.64**

structure—stress displayed by the entire tooth structure including the applied bracket. dentine—stress displayed by the dentine–cementum component of the tooth structure. a—root apical third, m—root middle third, c—root cervical third, C—crown.

Herein, the quantitative results were lower (i.e., 890.4 KPa, rotation, 8 mm loss, 0.6 N; 1.78 MPa rotation, 8 mm loss, 1.2 N) than the acknowledged dental components' physical properties.

Since all three applied forces showed similar qualitative stress displays and increasing quantitative results, the assumed applied boundary conditions (isotropy, linear elasticity, and homogeneity) are correct up to 2.4 N, if the Tresca failure criterion (for ductile non-homogenous materials) is employed.

4. Discussion

The present numerical analysis (eighty-one 3D models and 810 FEA simulations) assessed the absorption–dissipation ability of dental tissues under three forces (0.6, 1.2, and 2.4 N), and five most used orthodontic movements during 0–8 mm periodontal breakdown. Here, the simulation is the first study of its kind to bring an original approach in the dental studies field and new data with impact over clinical perspective. The absorption–dissipation ability of tooth as a single-stand structure was biomechanically recognized [1–3,11,14,48], and not yet investigated except for our previous research [2,3,9,10,48].

Additionally, by applying a third force (of 2.4 N), the correctness of using the assumptions of isotropy, linear elasticity, and homogeneity in FEA studies of dental tissues was assessed.

The biomechanical behavioral assessment following the progressive reduction in stress is individually displayed in each model's component. There was a visible progressive quantitative stress increase in all five movements strictly correlated with bone loss.

In both intact and reduced periodontium from the total amount of stress applied on and around the stainless-steel bracket base, only a constant percentage reached the alveolar bone socket (9.6–20% in 0 mm loss up to 36.73–50.04% in 8 mm loss), PDL (0.29–1.2% in 0 mm loss up to 2.24–8.37% in 8 mm loss), NVB (0.22–0.57% in 0 mm loss up to 0.32–0.69% in 8 mm loss), and dental pulp (0.02–0.05% in 0 mm up to 0.02–0.12% in 8 mm loss). However, due to the internal micro-architecture [1,11,13], the dentine component displayed an increase in variable percentage values which is correlated with the progression of periodontal breakdown (8.98–39.67% in 0 mm loss, 15.57–49.57% in 1 mm loss up to 58.35–92.9% in 8 mm loss).

The comparison between stresses displayed in the tooth with bracket and tooth without bracket showed a limited absorption–dissipation ability of stainless-steel stress bracket (15.48–18.73% in 0 mm, 16.43–18.16% in 1 mm loss up to 4.02–16.35% in 8 mm loss) except for translation which displayed doubled values (probably due to the movement's biomechanical specificity). The enamel component (comparison between tooth without bracket and coronal dentine) displayed a higher absorption–dissipation ability (50.29–62.26% in 0 mm, 49.09–62.26% in 1 mm loss up to 38.53–65.44% in 8 mm loss) than bracket. There is little difference (i.e., % of stress) at root level between the three structures (tooth with bracket, tooth without bracket, and dentine), the main differences being visible only in coronal part (where the main absorption–dissipation seems to take place).

Thus, the largest absorption–dissipation is performed by dentine (i.e., approx. 40–93%) and enamel (i.e., approx. 40–65%) components, while the stainless-steel bracket base has a limited ability (i.e., approx. 16%). Nevertheless, biomechanically, all three above components act similar to a single-stand structure that absorbs–dissipates most of the stresses produced by orthodontic loads, allowing for only a fraction of these stresses to be manifested in the circulatory sensitive tissues (i.e., approx. 0.3–8.4% in PDL, 0.2–0.7% in NVB, 0.02–0.12% in dental pulp, which are quantitatively under a physiological amount of 16 KPa of MHP). These agree with our previous reports about the absorption–dissipation ability found in PDL, dental pulp, NVB, tooth, and bone [5,6,9,10,16,48]. Regarding the bone alveolar socket, only approx. 10–20% in intact periodontium and 35–50% in 8 mm reduced periodontium reached the bone cervical third (with reduced circulatory vessels) and exceeded MHP, but with smaller percentages for apical and middle third where the circulatory component is better represented. The above biomechanical behavioral data were found for all three orthodontic loads since they displayed similar qualitative results and increased quantitative values (doubling for 1.2 N and quadrupling for 2.4 N).

A previous research [2,3,9,10,48] of our team (0.5–1.2 N of force, five movements, Tresca criteria, intact and reduced periodontium) reported a tooth structure absorption–dissipation ability of approx. 85% of stresses before reaching circulatory sensitive tissues (i.e., 86.66–97.5% dissipation before reaching PDL, 98% before reaching NVB, and 99.6–99.94% before reaching pulp) similar to the research herein.

Thus, the herein numerical simulation confirmed that 0.6–1.2 N are safe for application in intact periodontium, producing only minor limited ischemic and resorptive risks especially in the cervical third of PDL and bone alveolar socket, which is also in agreement with previous reports [5,6,9,10,16,48]. Nevertheless, in reduced periodontium, the same amounts of force increased ischemic and resorptive risks for radicular dentine and PDL, which are strictly correlated with the periodontal breakdown process, as previously reported [5,6,9,10,16,48]. This FEA simulation confirmed the importance of support tissues in biomechanical orthodontic behavior and the need to reduce orthodontic loads applied after 4 mm bone loss (to 0.2–0.6 N) to eliminate ischemic and resorptive risks, as previously recommended [5,6,9,10,16,48]. Therefore, the maximum force safely applied in these tissues should be the one that is safer for the weakest component (i.e., PDL and NVB). The 2.4 N force displayed in intact periodontium, for intrusion and extrusion, PDL cervical third stresses of 20.88–26.82 KPa exceeded the 16 KPa of MHP (prone to ischemic and resorptive risks), while in the other three movements the stresses were 3–4.5 times higher.

The above biomechanical behavior is due to the physical properties and internal micro-architecture of each tissular component. In both our previous [5,6,9,10,16,48] and other studies [1,2,7,8,11–15,17,18,51], dental tissues were reported to resemble ductile materials (i.e., elastic deformation with recovering of original form). Besides the main ductile nature, each one of these materials possesses a certain amount of brittle mode flow [5,6,9,10,16,48] (i.e., small deformation with cracking and destructions).

Enamel, due to its internal micro-architecture that is made of hydroxyapatite, was seen as brittle-like [1,11]. Nevertheless, this behavior is not clinically sustained (no cracking or destruction). Here, simulations confirmed very good absorption–dissipation deformation ability (i.e., 40–65%) and dentine resemblance (40–93%), thus being a ductile-like material, in agreement with a previous report [9]. Herein, the simulation is the first of its kind that scientifically proves that the enamel resembles a ductile material (confirming clinical knowledge) and is of extreme importance for the numerical studies (i.e., selection of failure criteria and boundary conditions). Moreover, it is the first FEA study to scientifically confirm the clinical knowledge about the tooth absorption–dissipation ability as a single-stand structure.

The other aim of the simulation herein was to assess the correctness of the boundary conditions' assumptions of isotropy, linear elasticity, and homogeneity for dental tissues when loads higher than 1 N loads were investigated. The results showed that qualitatively displayed stress was similar for all three loads, while quantitatively displayed stress increased (doubling for 1.2 N and quadrupling for 2.4 N). Thus, it seems that up to 2.4 N these assumptions can be used in FEA studies and obtain correct results. We must emphasize that these assumptions were investigated only under Tresca failure criteria (designed for non-homogenous ductile materials with a certain brittle flow mode). Moreover, both qualitative and quantitative results agreed with clinical and numerical data [2–6,9,10,16,48]. The explanation for this biomechanical behavior is that the displacements and deformations of tooth and surrounding tissues are extremely small, and thus the mechanical principles are compiled (i.e., under 1 N and small displacements all materials show linear elasticity and isotropy).

Since the simulation herein is the first of this type, the only possible correlation besides our previous research [5,6,9,10,16,48] was to indirectly compare the results with similar numerical studies [19–47] that assessed various components of dental tissues. The employed failure criterion was Von Mises (overall stress, for homogenous ductile-like materials), since no Tresca (shear stress, for non-homogenous ductile-like materials having a brittle flow mode) studies were found. Both criteria are mathematically similar, with Tresca quantitative results being 15–30% higher when compared with Von Mises (thus, correlations are acceptable). Most of the studies had similar boundary conditions with those in [19–47]. These comparisons assessed both qualitative behavioral stress display and quantitative results, which are correlated with physiological MHP (to confirm the amounts).

Merdji et al. [44] (lower third molar, intact periodontium, single model, sample size of one, Von Mises criteria, intrusion: 10 N, tipping/translation: 3 N, bone: 142,305 elements, global element size: 0.25–1 mm), reported similar qualitative results (cervical third alveolar bone socket stress), but with an extension on both vestibular and lingual sides (due to the three rooted anatomical reconstructions that are closer to bone–implant models [19–27] than tooth models). By following anatomical correctness, we addressed this issue in the herein models. Merdji et al. [44] quantitatively reported 10.5 MPa for 10 N of intrusion, 11.5 MPa for 3 N of tipping, and 16.83 MPa for 3 N of translation for alveolar bone socket cervical third and higher than herein for cervical radicular dentine for translation 20.36 MPa, intrusion 18.36 MPa, tipping 19.62 MPa, while in our study 0.6 N produced 149.83 KPa/0.149 MPa (intrusion), 146.53 KPa/0.146 MPa (tipping), and 185.28 KPa/0.185 MPa (translation), and 2.4 N displayed 599.32 KPa/0.599 MPa (intrusion), 586.12 KPa/0.586 MPa (tipping), and 741.14 KPa/0.741 MPa (translation). It was assumed that these differences were due to boundary conditions (global element size 0.25–1 mm and 142,305 elements [44] vs. global

element size 0.08–0.116 mm and 5,117,355 elements herein) and models' anatomy (idealized third molar [44] vs. anatomically correct second premolar).

Field et al. [43] (intact periodontium, two models, sample size of two, Von Mises criteria, tipping: 0.35/0.5 N, canine model: 23,565 elements, incisor-canine-first premolar model: 32,812 element, global element size: 1.2 mm) reported qualitative resembling results (as extension and topography—in bone, PDL, and radicular dentine). Nevertheless, it must be emphasized that their color-coded results were red—orange in the entire stress areas (high ischemic and resorptive risks) for light forces of 0.35 N, that clinically is not true. They also reported PDL quantitative stresses of 32–324.5 KPa, exceeding MHP signaling high resorptive risks, in total disagreement with herein and clinical data.

In intact periodontium, both Maravic et al. [49] (single simplified model of second upper premolar, intrusion) and Huang et al. [50] (single simplified model of first lower premolar, intrusion) reported comparable qualitative but higher quantitative results.

Hohmann et al. [37,38] (intact periodontium, one model, sample size of one, hydrostatic pressure criteria, maxillary first molar, intrusion: 0.5–1 N, PDL: 195,881–215,887 elements, tooth: 71,114–74,777 elements) reported maximum stresses of 9.95e-00TPa in the entire radicular dentine apical third, suggesting extended resorptive risks, in total disagreement with herein and contradicting clinical data. Moreover, the hydrostatic pressure criterion was specially designed for liquids (with no shear stress), thus its employment in dental tissues is not correct, as proven in other reports [3,9,48].

Shaw et al. [29] (upper incisor, intact periodontium, one model, sample size of one, Von Mises criteria, intrusion, extrusion, tipping, translation, and rotation, model: 11,924 elements and 20,852 nodes) reported lower amounts of alveolar bone socket and radicular dentine cervical stress as well as intrusion and extrusion to be more stressful than rotation and tipping, in total disagreement with herein (most likely due to boundary condition differences).

Shetty et al. [42] (upper first molar, intact periodontium, one model, sample size of one, Von Mises criteria, intrusion and tipping: 150 N, model: 30,838 nodes and 167,089 elements) quantitatively reported 1.33–1.95 MPa for intrusion and 2.16–8.15 MPa for tipping, and tipping to be more stressful than intrusion (in agreement with herein), but qualitatively displaying extended stress areas in the entire alveolar socket (in disagreement with herein).

The common issues found in these numerical studies [19–47] were the lack of correlation quantitative results of MHP, absence of scientifical motivation for employing a certain failure criterion (most studies), and biomechanical and physical mechanical explanations of boundary conditions when using higher loads.

Perrez et al. [30] partially approached these issues in endodontic root canal filling (concentrating on the brittleness aspect of root filling) but without any mention of Tresca or homogeneity/non-homogeneity, and linear- non-linear issues.

Comparative studies [2,3,9,16,48] have proven that only Von Mises and Tresca criteria supply correct results close to clinical data. Both criteria are specially designed for ductile materials, with Von Mises (overall stress) for homogenous materials and Tresca (shear stress) for non-homogenous materials with a brittle flow mode. By employing Tresca (maximum shear stress) criteria, the non-homogeneity nature of dental tissues was approached.

Multiple numerical studies by employing the hydrostatic pressure criteria (specially designed for liquids) and Ogdeon hyper-elastic model (specially designed for hyper-elastic rubbers) investigated an optimal PDL force in intact periodontium but with various and contradictive reports. Thus, Wu et al. [39–41] reported various optimal forces (in the range of 0.28–3.31 N) for canine, premolar, and lateral incisive, with significant differences for the same tooth (e.g., canine: rotation 1.7–2.1 N [41] and 3.31 N [39]; extrusion 0.38–0.4 N [41] and 2.3–2.6 N [40]; premolar: rotation 2.8–2.9 N [39]), much higher than 0.6–1.2 N reported by Proffit et al. [4] (0.1–1 N), and Hemanth et al. [32,33] (0.3–1 N).

Almost all FEA studies [19–47] employed the following boundary conditions: linear elasticity, isotropy, and homogeneity. Biomechanically, this is acceptable when subjected to small amounts of loads of up to 1 N. However, higher loads imply larger movements

and displacements, and the use of linear elasticity and the isotropy approach may not be correct [2,3,9,16,48]. A study of linearity vs. non-linearity was conducted by Hemanth et al. [32,33] in PDL of upper incisor subjected to 0.2–1 N of intrusion and tipping, which employed the S1 and S3 (brittle failure) criteria. The authors reported that up to 20–50% less quantitative applied force is needed for non-linearity vs. linearity. However, the employed failure criterion was of brittle-like material, while PDL is a ductile-like material; thus, their reports have accuracy issues. The use of failure criteria, which are specially designed for non-homogenous materials (as Tresca), deals with the homogeneity/non-homogeneity issue.

The main limit of an FEA numerical analysis is related to the fact that it cannot accurately reproduce clinical conditions. Clinically, there are no pure movements, but rather an association and combination; thus, the amount of stress displayed at tissular level could be smaller than the herein results. We foresee this limit and compensate through data interpretation (especially those close to the physiological limit). Nevertheless, the main advantage of numerical analysis is related to the fact that it can produce individual analyses of each tissular component (the only available method), while by changing the boundary conditions, it requires a small sample size. This is why most FEA studies [19–44] employed an acceptable sample size of one (one patient, one model, few simulations). To obtain correct and valid results, we approached this issue by using a larger sample size of nine (nine patients, eighty-one models, and 810 simulations), which was found to be superior to other numerical studies.

A limit could also be seen to the sample size of nine (i.e., nine patients). However, it must be emphasized that all of the previous numerical studies used a sample size of one (one patient with one FEA 3D model and only few simulations), while this study used 81 3D models and 810 numerical simulations. The FEA method allows for multiple changes in the physical properties and boundary conditions of the models, allowing for many simulations over the same models; thereby supplying reliable results even if a low number of models is used.

A good example of these changes is represented in our study by the tissular reconstruction of missing tissues (bone and PDL) and by the reduction of 1 mm to simulate various levels of bone loss (small enough to be numerically quantifiable and clinically relevant, since 1 mm is considered to be clinically relevant in both periodontics and orthodontics). It must be emphasized that if a large amount of bone loss occurs, the chances of keeping the tooth's functionality reduces, and thus the viability of keeping it in the oral cavity.

Most FEA analyses fasten the process by employing anatomical simplified models. Our approach was the manual reconstruction segmentation process (automated detection software missed some areas). Thus, our intact periodontium models had 5.06–6.05 million C3D4 tetrahedral elements, 0.97–1.07 million nodes, and a global element size of 0.08–0.116 mm, no error element, and only a limited number of elements. When compared with other FEA analyses, a lower number of elements and nodes and higher global element size were used, with influence over results accuracy: 142,305 elements [44], 23,565–32,812 elements [43], 30,838 nodes and 167,089 elements [42], 148,097 elements and 239,666 nodes [32,33], 11,924 elements and 20,852 nodes [29], and higher global element size of 1.2 mm [43] and 0.25–1 mm [44].

To confirm numerical simulations, correct results must be compared and correlated with both physiological constants, with clinical data, and other studies. Herein, the analysis approached the above-mentioned issues by correlating the results with MHP found in periodontal and dental pulp circulatory vessels and known clinical data.

5. Conclusions

1. The largest absorption–dissipation is performed by dentine (i.e., approx. 40–93%) and enamel (i.e., approx. 40–65%) components, while the stainless-steel bracket base has a limited ability (i.e., approx. 16%).
2. The main absorption–dissipation of stresses takes place in coronal part since there is little difference (i.e., % of stress) at root level between the three structures (i.e., tooth

with bracket, tooth without bracket, and dentine), the main differences being visible only in coronal part.
3. Enamel, dentine, and stainless-steel bracket biomechanically behave as a single-stand structure, allowing for only a limited fraction of stresses to reach the circulatory sensitive tissues (i.e., approx. 0.3–8.4% in PDL, 0.2–0.7% in NVB, 0.02–0.12% in dental pulp, and quantitatively under the physiological amount of 16 KPa of MHP).
4. Enamel component displayed dentine resemblance of absorption–dissipation ability, thus being proven to resemble more ductile materials (with a certain brittle flow mode).
5. Tooth behaves as a single-stand structure showing the highest absorption–dissipation ability among dental tissues.
6. These numerical simulations confirmed clinical biomechanical knowledge, showing that 0.6–1.2 N of force are safe to be applied in intact periodontium, while for reduced periodontium, forces higher than 0.6 N are prone to resorptive and ischemic risks.
7. For reducing ischemic and resorptive risks, after 4 mm of bone loss, 0.2–0.6 N of force are recommended, to keep stresses under the 16 KPa physiological limit.
8. The rotational and translational movements were the most stressful, followed by tipping.
9. Both intrusion and extrusion supplied similar quantitative and quantitative results.
10. Forces of 0.6 N, 1.2 N, and 2.4 N displayed similar qualitative results for all movements and bone levels, while quantitative results doubled for 1.2 N and quadrupled for 2.4 N when compared with 0.6 N.
11. The employment of isotropy, linear elasticity, and homogeneity as assumed boundary conditions for the study of dental tissues seems to be correct when Tresca criterion (for non-homogenous materials) is used, for loads up to 2.4 N.

Author Contributions: Conceptualization, R.-A.M.; methodology, R.-A.M.; software, R.-A.M.; validation, R.-A.M. and C.D.O.; formal analysis, R.-A.M.; investigation, R.-A.M.; resources, R.-A.M.; data curation, R.-A.M.; writing—original draft preparation, R.-A.M.; writing—review and editing, R.-A.M., A.G.D. and C.D.O.; visualization, supervision, project administration, R.-A.M., A.G.D. and C.D.O.; funding acquisition, R.-A.M., A.G.D. and C.D.O. All authors have read and agreed to the published version of the manuscript.

Funding: The authors were the funders of this research project.

Institutional Review Board Statement: The research protocol has been approved by the Ethical Committee of the University of Medicine (158/2.04.2018).

Informed Consent Statement: Informed oral consent was obtained from all subjects involved in the study.

Data Availability Statement: Data are contained within the article.

Conflicts of Interest: The authors declare that they have no conflicts of interest.

References

1. Chun, K.; Choi, H.; Lee, J. Comparison of mechanical property and role between enamel and dentin in the human teeth. *J. Dent. Biomech.* **2014**, *5*, 1758736014520809. [CrossRef]
2. Moga, R.A.; Buru, S.M.; Olteanu, C.D. Assessment of the Best FEA Failure Criteria (Part II): Investigation of the Biomechanical Behavior of Dental Pulp and Apical-Neuro-Vascular Bundle in Intact and Reduced Periodontium. *Int. J. Environ. Res. Public Health* **2022**, *19*, 15635. [CrossRef]
3. Moga, R.A.; Buru, S.M.; Olteanu, C.D. Assessment of the Best FEA Failure Criteria (Part I): Investigation of the Biomechanical Behavior of PDL in Intact and Reduced Periodontium. *Int. J. Environ. Res. Public Health* **2022**, *19*, 12424. [CrossRef] [PubMed]
4. Proffit, W.R.; Fields, H.W.; Sarver, D.M.; Ackerman, J.L. *Contemporary Orthodontics*, 5th ed.; Elsevier: St. Louis, MO, USA, 2012.
5. Moga, R.A.; Olteanu, C.D.; Botez, M.; Buru, S.M. Assessment of the Maximum Amount of Orthodontic Force for Dental Pulp and Apical Neuro-Vascular Bundle in Intact and Reduced Periodontium on Bicuspids (Part II). *Int. J. Environ. Res. Public Health* **2023**, *20*, 1179. [CrossRef] [PubMed]
6. Moga, R.A.; Olteanu, C.D.; Botez, M.; Buru, S.M. Assessment of the Maximum Amount of Orthodontic Force for PDL in Intact and Reduced Periodontium (Part I). *Int. J. Environ. Res. Public Health* **2023**, *20*, 1889. [CrossRef]

7. Elsaka, S.E.; Hammad, S.M.; Ibrahim, N.F. Evaluation of stresses developed in different bracket-cement-enamel systems using finite element analysis with in vitro bond strength tests. *Prog. Orthod.* **2014**, *15*, 33. [CrossRef] [PubMed]
8. Algera, T.J.; Feilzer, A.J.; Prahl-Andersen, B.; Kleverlaan, C.J. A comparison of finite element analysis with in vitro bond strength tests of the bracket-cement-enamel system. *Eur. J. Orthod.* **2011**, *33*, 608–612. [CrossRef] [PubMed]
9. Moga, R.A.; Olteanu, C.D.; Buru, S.M.; Botez, M.D.; Delean, A.G. Finite Elements Analysis of Biomechanical Behavior of the Bracket in a Gradual Horizontal Periodontal Breakdown; A Comparative Analysis of Multiple Failure Criteria. *Appl. Sci.* **2023**, *13*, 9480. [CrossRef]
10. Moga, R.A.; Olteanu, C.D.; Botez, M.D.; Buru, S.M. Assessment of the Orthodontic External Resorption in Periodontal Breakdown-A Finite Elements Analysis (Part I). *Healthcare* **2023**, *11*, 1447. [CrossRef]
11. Giannini, M.; Soares, C.J.; de Carvalho, R.M. Ultimate tensile strength of tooth structures. *Dent. Mater. Off. Publ. Acad. Dent. Mater.* **2004**, *20*, 322–329. [CrossRef]
12. Kailasam, V.; Rangarajan, H.; Easwaran, H.N.; Muthu, M.S. Proximal enamel thickness of the permanent teeth: A systematic review and meta-analysis. *Am. J. Orthod. Dentofac. Orthop. Off. Publ. Am. Assoc. Orthod. Its Const. Soc. Am. Board Orthod.* **2021**, *160*, 793–804.e3. [CrossRef]
13. Konishi, N.; Watanabe, L.G.; Hilton, J.F.; Marshall, G.W.; Marshall, S.J.; Staninec, M. Dentin shear strength: Effect of distance from the pulp. *Dent. Mater. Off. Publ. Acad. Dent. Mater.* **2002**, *18*, 516–520. [CrossRef]
14. Jang, Y.; Hong, H.T.; Roh, B.D.; Chun, H.J. Influence of apical root resection on the biomechanical response of a single-rooted tooth: A 3-dimensional finite element analysis. *J. Endod.* **2014**, *40*, 1489–1493. [CrossRef]
15. Burr, D.B. Why bones bend but don't break. *J. Musculoskelet. Neuronal Interact.* **2011**, *11*, 270–285. [PubMed]
16. Moga, R.A.; Olteanu, C.D.; Buru, S.M.; Botez, M.D.; Delean, A.G. Cortical and Trabecular Bone Stress Assessment during Periodontal Breakdown-A Comparative Finite Element Analysis of Multiple Failure Criteria. *Medicina* **2023**, *59*, 1462. [CrossRef] [PubMed]
17. Hart, N.H.; Nimphius, S.; Rantalainen, T.; Ireland, A.; Siafarikas, A.; Newton, R.U. Mechanical basis of bone strength: Influence of bone material, bone structure and muscle action. *J. Musculoskelet. Neuronal Interact.* **2017**, *17*, 114–139. [PubMed]
18. Wu, V.; Schulten, E.; Helder, M.N.; Ten Bruggenkate, C.M.; Bravenboer, N.; Klein-Nulend, J. Bone vitality and vascularization of mandibular and maxillary bone grafts in maxillary sinus floor elevation: A retrospective cohort study. *Clin. Implant. Dent. Relat. Res.* **2023**, *25*, 141–151. [CrossRef] [PubMed]
19. Prados-Privado, M.; Martínez-Martínez, C.; Gehrke, S.A.; Prados-Frutos, J.C. Influence of Bone Definition and Finite Element Parameters in Bone and Dental Implants Stress: A Literature Review. *Biology* **2020**, *9*, 224. [CrossRef] [PubMed]
20. Tawara, D.; Nagura, K. Predicting changes in mechanical properties of trabecular bone by adaptive remodeling. *Comput. Methods Biomech. Biomed. Eng.* **2017**, *20*, 415–425. [CrossRef] [PubMed]
21. Yamanishi, Y.; Yamaguchi, S.; Imazato, S.; Nakano, T.; Yatani, H. Effects of the implant design on peri-implant bone stress and abutment micromovement: Three-dimensional finite element analysis of original computer-aided design models. *J. Periodontol.* **2014**, *85*, e333–e338. [CrossRef]
22. Pérez-Pevida, E.; Brizuela-Velasco, A.; Chávarri-Prado, D.; Jiménez-Garrudo, A.; Sánchez-Lasheras, F.; Solaberrieta-Méndez, E.; Diéguez-Pereira, M.; Fernández-González, F.J.; Dehesa-Ibarra, B.; Monticelli, F. Biomechanical Consequences of the Elastic Properties of Dental Implant Alloys on the Supporting Bone: Finite Element Analysis. *BioMed Res. Int.* **2016**, *2016*, 1850401. [CrossRef]
23. Shash, Y.H.; El-Wakad, M.T.; Eldosoky, M.A.A.; Dohiem, M.M. Evaluation of stress and strain on mandible caused using "All-on-Four" system from PEEK in hybrid prosthesis: Finite-element analysis. *Odontology* **2022**, *111*, 618–629. [CrossRef]
24. Park, J.M.; Kim, H.J.; Park, E.J.; Kim, M.R.; Kim, S.J. Three dimensional finite element analysis of the stress distribution around the mandibular posterior implant during non-working movement according to the amount of cantilever. *J. Adv. Prosthodont.* **2014**, *6*, 361–371. [CrossRef]
25. Cicciù, M.; Cervino, G.; Milone, D.; Risitano, G. FEM Investigation of the Stress Distribution over Mandibular Bone Due to Screwed Overdenture Positioned on Dental Implants. *Materials* **2018**, *11*, 1512. [CrossRef]
26. Aunmeungtong, W.; Khongkhunthian, P.; Rungsiyakull, P. Stress and strain distribution in three different mini dental implant designs using in implant retained overdenture: A finite element analysis study. *ORAL Implantol.* **2016**, *9*, 202–212.
27. Merdji, A.; Bachir Bouiadjra, B.; Achour, T.; Serier, B.; Ould Chikh, B.; Feng, Z.O. Stress analysis in dental prosthesis. *Comput. Mater. Sci.* **2010**, *49*, 126–133. [CrossRef]
28. Vikram, N.R.; Senthil Kumar, K.S.; Nagachandran, K.S.; Hashir, Y.M. Apical stress distribution on maxillary central incisor during various orthodontic tooth movements by varying cemental and two different periodontal ligament thicknesses: A FEM study. *Indian J. Dent. Res. Off. Publ. Indian Soc. Dent. Res.* **2012**, *23*, 213–220. [CrossRef] [PubMed]
29. Shaw, A.M.; Sameshima, G.T.; Vu, H.V. Mechanical stress generated by orthodontic forces on apical root cementum: A finite element model. *Orthod. Craniofacial Res.* **2004**, *7*, 98–107. [CrossRef]
30. Perez-Gonzalez, A.; Iserte-Vilar, J.L.; Gonzalez-Lluch, C. Interpreting finite element results for brittle materials in endodontic restorations. *Biomed. Eng. Online* **2011**, *10*, 44. [CrossRef]
31. McCormack, S.W.; Witzel, U.; Watson, P.J.; Fagan, M.J.; Groning, F. Inclusion of periodontal ligament fibres in mandibular finite element models leads to an increase in alveolar bone strains. *PLoS ONE* **2017**, *12*, e0188707. [CrossRef] [PubMed]

32. Hemanth, M.; Deoli, S.; Raghuveer, H.P.; Rani, M.S.; Hegde, C.; Vedavathi, B. Stress Induced in the Periodontal Ligament under Orthodontic Loading (Part I): A Finite Element Method Study Using Linear Analysis. *J. Int. Oral Health JIOH* **2015**, *7*, 129–133.
33. Hemanth, M.; Deoli, S.; Raghuveer, H.P.; Rani, M.S.; Hegde, C.; Vedavathi, B. Stress Induced in Periodontal Ligament under Orthodontic Loading (Part II): A Comparison of Linear Versus Non-Linear Fem Study. *J. Int. Oral Health JIOH* **2015**, *7*, 114–118. [PubMed]
34. Reddy, R.T.; Vandana, K.L. Effect of hyperfunctional occlusal loads on periodontium: A three-dimensional finite element analysis. *J. Indian Soc. Periodontol.* **2018**, *22*, 395–400. [PubMed]
35. Jeon, P.D.; Turley, P.K.; Moon, H.B.; Ting, K. Analysis of stress in the periodontium of the maxillary first molar with a three-dimensional finite element model. *Am. J. Orthod. Dentofac. Orthop. Off. Publ. Am. Assoc. Orthod. Its Const. Soc. Am. Board Orthod.* **1999**, *115*, 267–274. [CrossRef] [PubMed]
36. Jeon, P.D.; Turley, P.K.; Ting, K. Three-dimensional finite element analysis of stress in the periodontal ligament of the maxillary first molar with simulated bone loss. *Am. J. Orthod. Dentofac. Orthop. Off. Publ. Am. Assoc. Orthod. Its Const. Soc. Am. Board Orthod.* **2001**, *119*, 498–504. [CrossRef] [PubMed]
37. Hohmann, A.; Wolfram, U.; Geiger, M.; Boryor, A.; Kober, C.; Sander, C.; Sander, F.G. Correspondences of hydrostatic pressure in periodontal ligament with regions of root resorption: A clinical and a finite element study of the same human teeth. *Comput. Methods Programs Biomed.* **2009**, *93*, 155–161. [PubMed]
38. Hohmann, A.; Wolfram, U.; Geiger, M.; Boryor, A.; Sander, C.; Faltin, R.; Faltin, K.; Sander, F.G. Periodontal ligament hydrostatic pressure with areas of root resorption after application of a continuous torque moment. *Angle Orthod.* **2007**, *77*, 653–659. [CrossRef] [PubMed]
39. Wu, J.; Liu, Y.; Li, B.; Wang, D.; Dong, X.; Sun, Q.; Chen, G. Numerical simulation of optimal range of rotational moment for the mandibular lateral incisor, canine and first premolar based on biomechanical responses of periodontal ligaments: A case study. *Clin. Oral Investig.* **2021**, *25*, 1569–1577. [CrossRef]
40. Wu, J.; Liu, Y.; Wang, D.; Zhang, J.; Dong, X.; Jiang, X.; Xu, X. Investigation of effective intrusion and extrusion force for maxillary canine using finite element analysis. *Comput. Methods Biomech. Biomed. Eng.* **2019**, *22*, 1294–1302. [CrossRef]
41. Wu, J.L.; Liu, Y.F.; Peng, W.; Dong, H.Y.; Zhang, J.X. A biomechanical case study on the optimal orthodontic force on the maxillary canine tooth based on finite element analysis. *J. Zhejiang Univ. Sci. B* **2018**, *7*, 535–546. [CrossRef]
42. Shetty, B.; Fazal, I.; Khan, S.F. FEA analysis of Normofunctional forces on periodontal elements in different angulations. *Bioinformation* **2022**, *18*, 245–250. [CrossRef] [PubMed]
43. Field, C.; Ichim, I.; Swain, M.V.; Chan, E.; Darendeliler, M.A.; Li, W.; Li, Q. Mechanical responses to orthodontic loading: A 3-dimensional finite element multi-tooth model. *Am. J. Orthod. Dentofac. Orthop. Off. Publ. Am. Assoc. Orthod. Its Const. Soc. Am. Board Orthod.* **2009**, *135*, 174–181. [CrossRef] [PubMed]
44. Merdji, A.; Mootanah, R.; Bachir Bouiadjra, B.A.; Benaissa, A.; Aminallah, L.; Ould Chikh el, B.; Mukdadi, S. Stress analysis in single molar tooth. *Mater. Sci. Eng. C Mater. Biol. Appl.* **2013**, *33*, 691–698. [CrossRef] [PubMed]
45. Wu, A.T.; Turk, T.; Colak, C.; Elekdag-Turk, S.; Jones, A.S.; Petocz, P.; Darendeliler, M.A. Physical properties of root cementum: Part 18. The extent of root resorption after the application of light and heavy controlled rotational orthodontic forces for 4 weeks: A microcomputed tomography study. *Am. J. Orthod. Dentofac. Orthop. Off. Publ. Am. Assoc. Orthod. Its Const. Soc. Am. Board Orthod.* **2011**, *139*, e495–e503. [CrossRef]
46. Chan, E.; Darendeliler, M.A. Physical properties of root cementum: Part 5. Volumetric analysis of root resorption craters after application of light and heavy orthodontic forces. *Am. J. Orthod. Dentofac. Orthop. Off. Publ. Am. Assoc. Orthod. Its Const. Soc. Am. Board Orthod.* **2005**, *127*, 186–195. [CrossRef]
47. Zhong, J.; Chen, J.; Weinkamer, R.; Darendeliler, M.A.; Swain, M.V.; Sue, A.; Zheng, K.; Li, Q. In vivo effects of different orthodontic loading on root resorption and correlation with mechanobiological stimulus in periodontal ligament. *J. R. Soc. Interface* **2019**, *16*, 20190108. [CrossRef]
48. Moga, R.A.; Olteanu, C.D.; Daniel, B.M.; Buru, S.M. Finite Elements Analysis of Tooth-A Comparative Analysis of Multiple Failure Criteria. *Int. J. Environ. Res. Public Health* **2023**, *20*, 4133. [CrossRef]
49. Maravić, T.; Comba, A.; Mazzitelli, C.; Bartoletti, L.; Balla, I.; di Pietro, E.; Josić, U.; Generali, L.; Vasiljević, D.; Blažić, L.; et al. Finite element and in vitro study on biomechanical behavior of endodontically treated premolars restored with direct or indirect composite restorations. *Sci. Rep.* **2022**, *12*, 12671. [CrossRef]
50. Huang, L.; Nemoto, R.; Okada, D.; Shin, C.; Saleh, O.; Oishi, Y.; Takita, M.; Nozaki, K.; Komada, W.; Miura, H. Investigation of stress distribution within an endodontically treated tooth restored with different restorations. *J. Dent. Sci.* **2022**, *17*, 1115–1124. [CrossRef]
51. Gupta, M.; Madhok, K.; Kulshrestha, R.; Chain, S.; Kaur, H.; Yadav, A. Determination of stress distribution on periodontal ligament and alveolar bone by various tooth movements—A 3D FEM study. *J. Oral Biol. Craniofacial Res.* **2020**, *10*, 758–763. [CrossRef]